EFFECTS OF EXERCISE AND OBESITY ON PANCREATIC VASCULATURE IN MICE

Outi Hasu

Master`s Thesis in Exercise Physiology
Faculty of Sport and Health Sciences
University of Jyväskylä
Autumn 2024
Supervisors: Riikka Kivelä, Kialiina Tonttila
Additional support: Vasco Fachada, Bettina Hutz

TIIVISTELMÄ

Hasu, O. 2024. Liikunnan ja lihavuuden vaikutukset hiirten haiman verisuonistoon. Liikuntatieteellinen tiedekunta, Jyväskylän yliopisto, liikuntafysiologian pro gradu -tutkielma, 64 s., 3 liitettä.

Tausta. Kardiometaboliset sairaudet, kuten sydän- ja verisuonisairaudet, lihavuus ja tyypin 2 diabetes (T2D), ovat maailman yleisimpiä kuolinsyitä. Lihavuus ja siihen liittyvät aineenvaihduntasairaudet, kuten T2D, voivat heikentää hiussuoniston toimintaa eri elimissä. Koska hiussuonet mahdollistavat solujen ja veren välisen ravintoaineiden sekä hengitysilman kaasujen ja kuona-aineiden vaihdon, muutokset niiden morfologiassa ja määrässä voivat merkitsevästi vaikuttaa kudosten toimintaan, aineenvaihduntaan ja yleiseen hyvinvointiin. Sekä ihmis- että hiiritutkimuksissa on huomattu T2D aiheuttavan morfologisia muutoksia haiman saarekkeiden verisuonissa, kun taas muualla haimassa verisuonet ovat enimmäkseen muuttumattomia. Vaikka fyysisen aktiivisuuden on osoitettu vähentävän aiemmin mainittujen sairauksien riskiä ja liikunnan merkitys on laajalti tunnustettu, sen positiivisia vaikutuksia solutasolla ei vielä täysin ymmärretä. Näin ollen tutkimuksen tavoitteena oli selvittää hiirimallinnuksen avulla ylipainon ja liikunnan aiheuttamia muutoksia haiman hiusverisuonten tiheydessä ja pinta-alassa.

Menetelmät. Aikuiset C57BL/6J uroshiiret (n=40) jaettiin satunnaisesti neljään ryhmään: 1) hoikat liikkumattomat, 2) lihavat liikkumattomat, 3) hoikat liikkuvat, ja 4) lihavat liikkuvat. Lihavuus, hyperglykemia ja insuliiniresistenssi saatiin aikaan 18 viikon Western diet -ruokavaliolla. Liikuntaryhmille juokseminen mahdollistettiin kymmenennestä viikosta eteenpäin ja se jatkui aina tutkimuksen loppuun asti. Haimasta ja maksasta otetut ohutleikkeet värjättiin hematoksyliini-eosiinilla (H&E) ja immunofluoresenssin avulla. Haiman ohutleikkeiden kuva-analysointi tehtiin Fiji/ImageJ–kuva-analyysiohjelmalla. Parillista t-testiä käytettiin intervention ennen ja jälkeen -tulosten tulkintaan ja yksisuuntaista ANOVA-testiä käytettiin määrittämään erot eri hiiriryhmien välillä.

Tulokset. Lihavien hiiriryhmien H&E-värjätyissä maksaleikkeissä rasvaa oli kertynyt selvästi enemmän hoikkiin hiiriin verrattuna. Lisäksi liikunnan huomattiin vähentäneen rasvan kertymistä maksaan. Haiman saarekkeiden verisuonissa ei havaittu merkitseviä muutoksia. Haiman eksokriinisessä kudoksessa verisuonten tiheys ja verisuonten suhde tumien lukumäärään olivat yleisesti ottaen suurempia lihavien hiirten ryhmissä verrattuna hoikkiin hiiriin. Lihavilla, liikuntaa harrastamattomilla hiirillä oli merkitsevästi suurempi verisuonten tiheys kuin hoikilla hiirillä. Lisäksi lihavilla liikuntaa harrastaneilla hiirillä oli merkitsevästi suurempi verisuonten tiheys kuin hoikilla liikkumattomilla hiirillä. Haiman saarekkeiden verisuonten tiheys, verisuonten suhteellinen osuus pinta-alasta ja Feret'n halkaisija olivat merkitsevästi suurempia kuin haiman eksokriinisen kudoksen.

Johtopäätökset. Lihavilla hiirillä oli havaittavissa taipumusta kapillaarien laajenemiseen haiman saarekkeissa. Pidempi interventiojakso voisi paljastaa merkitsevämpiä muutoksia. Lihavien hiirten eksokriinisessä kudoksessa havaittu suurentunut verisuonten tiheys ja toisaalta pienempi Feret'n halkaisija voivat viitata angiogeneesiin, jossa yksi verisuoni jakautuu kahdeksi. Liikunnan vaikutus verisuonistoon oli vähäinen. Tulevaisuudessa tulisi ottaa huomioon ihmisverisuoniin kasautuvien amyloidikertymien vaikutus haiman verisuonistoon.

Asiasanat: haima, haiman verisuonet, hiusverisuonten tiheys, tyypin 2 diabetes, haiman saareke, Langerhansin saareke

ABSTRACT

Hasu, O. 2024. Effects of Exercise and Obesity on Pancreatic Vasculature in Mice. Faculty of Sport and Health Sciences, University of Jyväskylä, Master's thesis in Exercise Physiology, 64 pp., 3 appendices.

Background. Cardiometabolic diseases, such as cardiovascular disease, obesity and type 2 diabetes, are the leading causes of death globally. Obesity and its associated metabolic diseases, like type 2 diabetes, can impair the microcirculation in different organs. Since vascular capillaries are the main site for substance exchange between cells and the vasculature, changes in their morphology and number can have serious effects on tissue function, metabolic health, and overall well-being. In the pancreas, type 2 diabetes has been shown to lead to morphological changes in both human and rodent intra-islet vasculature, while the exocrine vasculature remains mostly unaltered. Also, although physical activity has been shown to reduce the risk of these diseases, and despite the recognition of the importance of exercise, its positive effects at the cellular level are not yet fully understood. Therefore, this thesis aimed to investigate the changes that obesity and exercise induce on pancreatic capillary density and capillary area both together and separately using a mouse model.

Methods. Adult C57BL/6J male mice (n=40) were randomized into four groups: 1) lean sedentary, 2) obese sedentary, 3) lean exercise, and 4) obese exercise. Obesity, hyperglycaemia and insulin resistance were induced using a Western diet for 18 weeks. Voluntary running for the exercise groups was started at ten weeks and lasted until the end of the study. Pancreas and liver sections were stained with haematoxylin-eosin (H&E) and with immunofluorescence. The image processing and analysis for pancreas sections were performed using Fiji/ImageJ software. A paired T-test was used to study changes between pre- and post-intervention and one-way ANOVA was used to determine differences between different mouse groups.

Results. In H&E-stained liver sections, obese mice had visibly more lipid accumulation than the lean mice. Also, exercise was shown to reduce the lipid accumulation in the liver. In pancreatic islet capillaries, no significant differences were observed. In pancreatic exocrine tissue, the capillary density and capillaries-to-nuclei ratio were generally higher in obese groups compared to lean groups. In more detail, the obese sedentary group had significantly higher capillary density than both lean groups, and the obese exercise group had significantly higher capillary density than the lean sedentary group. All in all, compared to exocrine tissue, the pancreatic islets exhibited significantly higher capillary density, capillary area relative to tissue area, and capillary Feret's diameter.

Conclusions. In islets, a trend toward possible capillary enlargement in obese groups suggests that subtle vascular changes might be occurring in response to high-fat feeding, and a longer intervention period could potentially reveal more pronounced effects. In exocrine tissue, significantly increased capillary density and slightly smaller Feret's diameter in obese mice could indicate intussusceptive angiogenesis. The effect of exercise on vasculature was minor in both areas of pancreas. In future studies, the influence of amyloid deposits should be considered.

Key words: Pancreas, Pancreatic Vasculature, Capillary Density, Type 2 Diabetes, Pancreatic islet, Islet of Langerhans

ABBREVIATIONS

ACSM	American College of Sports Medicine
ADA	American Diabetes Association
AMI	Acute Myocardial Infarction
AUC GTT	Area Under the Curve Glucose Tolerance Test
BM	Basement Membrane
BMI	Body Mass Index
CMD	Cardiometabolic Disease
DAPI	4′,6-Diamidino-2-Phenylindole
DXA	Dual-Energy X-Ray Absorptiometry
EC	Endothelial Cell
GTT	Glucose Tolerance Test
HbA1c	Glycated Haemoglobin
HFD	High Fat Diet
HIP	Human Islet Amyloid Polypeptide Rat Model
H&E	Haematoxylin-Eosin Staining
ICD	Islet Capillary Density
IR	Insulin Resistance
LFD	Low Fat Diet
OLETF	Otsuka Long-Evans Tokushima Fatty Rats
PBS	Phosphate Buffer Saline
PA	Physical Activity
PFA	Paraformaldehyde
RT	Room Temperature
SMC	Smooth Muscle Cell
TEM	Transmission Electron Microscope
TNT	Tris-NaCl-Tween Buffer
T2D	Type 2 Diabetes
UEA 1	Ulex Europaeus Agglutinin I lectin
WD	Western Diet
ZDF	Zucker Diabetic Fatty Rats

CONTENTS

Appendix 2: Immunofluorescence staining protocol for paraffin-embedded tissue sections.

Appendix 3: Fiji/ImageJ image analysis code for capillaries of pancreas sections.

1 INTRODUCTION

Cardiometabolic diseases (CMDs), such as obesity, atherosclerosis and type 2 diabetes (T2D), are among the leading causes of death in the world (Paavonsalo et al. 2020). According to a review by Galicia-Garcia et al. (2020), T2D is one of the most common metabolic disorders globally, with risk factors including both genetic and environmental factors, the latter being similar to those of other CMDs (de Waard et al. 2019). While genetics play a role in the development of T2D, it can often be prevented by addressing environmental risk factors such as obesity, low physical activity (PA), and unhealthy diet (Galicia-Garcia et al. 2020). Although PA has been shown to reduce the overall risk of developing any cardiovascular diseases (Cristi-Montero et al. 2019), including T2D, the mechanisms behind the positive impact of exercise are not yet fully understood.

According to Paavonsalo et al. (2020), CMDs can lead to both vascular dysfunction and changes in capillary density. However, these changes in capillary density appear to be organ-specific, causing morphological and functional alterations in some tissues but not in others (Paavonsalo et al. 2020). For example, obesity is associated with capillary rarefaction in muscle tissue (Paavonsalo et al. 2020), whereas studies on the pancreas show slightly different outcomes between human and rodent models (Brissova et al. 2015). Overall, the vasculature studies of pancreas indicate morphological changes in both human and rodent islet vasculature in T2D, while the vasculature in peri-islet and exocrine capillaries remains mostly unaltered (Brissova et al. 2015; Dai et al. 2013).

In general, exercise has been shown to influence vascular function and structure across various tissues (Green & Smith 2018). However, the existing literature on the effects of exercise on pancreatic vasculature is scarce – one might even say non-existent. Therefore, the aim of this thesis was to investigate the changes in pancreatic capillary density influenced by obesity and exercise, both together and separately, using a mouse model. Additionally, the staining protocol used in this thesis was optimized not only for pancreatic tissue, but also for liver tissue for use in future research.

2 OVERVIEW OF HUMAN VASCULATURE

Vascular system of the human body consists of numerous vessels that enable blood circulation throughout the body (Pugsley & Tabrizchi 2000). The key functions of this vascular system are as follows: 1) maintenance of homeostasis, 2) transportation of nutrients and oxygen from the circulation into tissues, and 3) removal of carbon dioxide and waste products from the tissues into the circulation (Paavonsalo et al. 2020). The blood vessels can be divided into arteries, arterioles, veins, venules, and capillaries, depending on their structure and function. From these five, arterioles, venules and capillaries constitute the microvasculature (Potente & Mäkinen 2017) which is the main site for substance exchange between cells and the vasculature (Guyton & Hall 2011, 157). The capillaries are the link between arterial and venous system (Pugsley & Tabrizchi 2000), and their approximate diameter ranges from 4 to 9 micrometres and hence, the blood cells can barely fit through them (Guyton & Hall 2011, 177).

Function of the vasculature. The human circulatory system can be divided into two parts: pulmonary circulation and systemic circulation. In pulmonary circulation, deoxygenated blood that is returned from the periphery to the right atrium of the heart is pumped to the lungs. There, the blood is oxygenated and then returned to the left atrium of the heart. (Guyton & Hall 2011, 157) From there, it then continues to systemic circulation where, in short, the oxygenated blood from the heart circulates through arteries and moves towards smaller arterioles and even smaller capillaries where the exchange of substances between cells and blood vessels takes place. From the capillaries the blood is then collected into venules and later into larger veins, bringing the now deoxygenated blood back to the heart and lungs to be re-oxygenated. (Potente & Mäkinen 2017)

Structure of vascular walls. The vascular wall consists of three distinct regions, here named in order from the inside to the outside: tunica intima, tunica media and tunica adventitia (Figure 1) (Pugsley & Tabrizchi 2000). The innermost layer, tunica intima, is the thinnest layer consisting of a single layer of endothelial cells (EC) mounted on a basement membrane (BM) (Pugsley & Tabrizchi 2000; Trimm & Red-Horse 2023). The second layer, tunica media, contains mainly smooth muscle cells (SMCs) and elastin fibres, and the third and outermost layer, tunica adventitia, is mainly composed of fibro-elastic connective tissue (Potente & Mäkinen 2017; Pugsley & Tabrizchi 2000). In terms of blood vessel type, the large arteries and veins are surrounded by

a continuous lining of ECs, BM and layers of SMCs whereas in capillaries, the ECs are especially organ-specifically differentiated to accommodate the specific needs of the tissue that they supply. Therefore, the capillary ECs can be either continuous, fenestrated or discontinuous, and they can have a varying amount of BM and pericyte coverage (Potente & Mäkinen 2017; Trimm & Red-Horse 2023). Pericytes are cells that belong to the same class of cells as SMCs, called mural cells (Richards, Raines & Attie 2010). Therefore, similar to SMCs, they provide support to blood vessels, and they have been reported to have contractile properties (Potente & Mäkinen 2017).

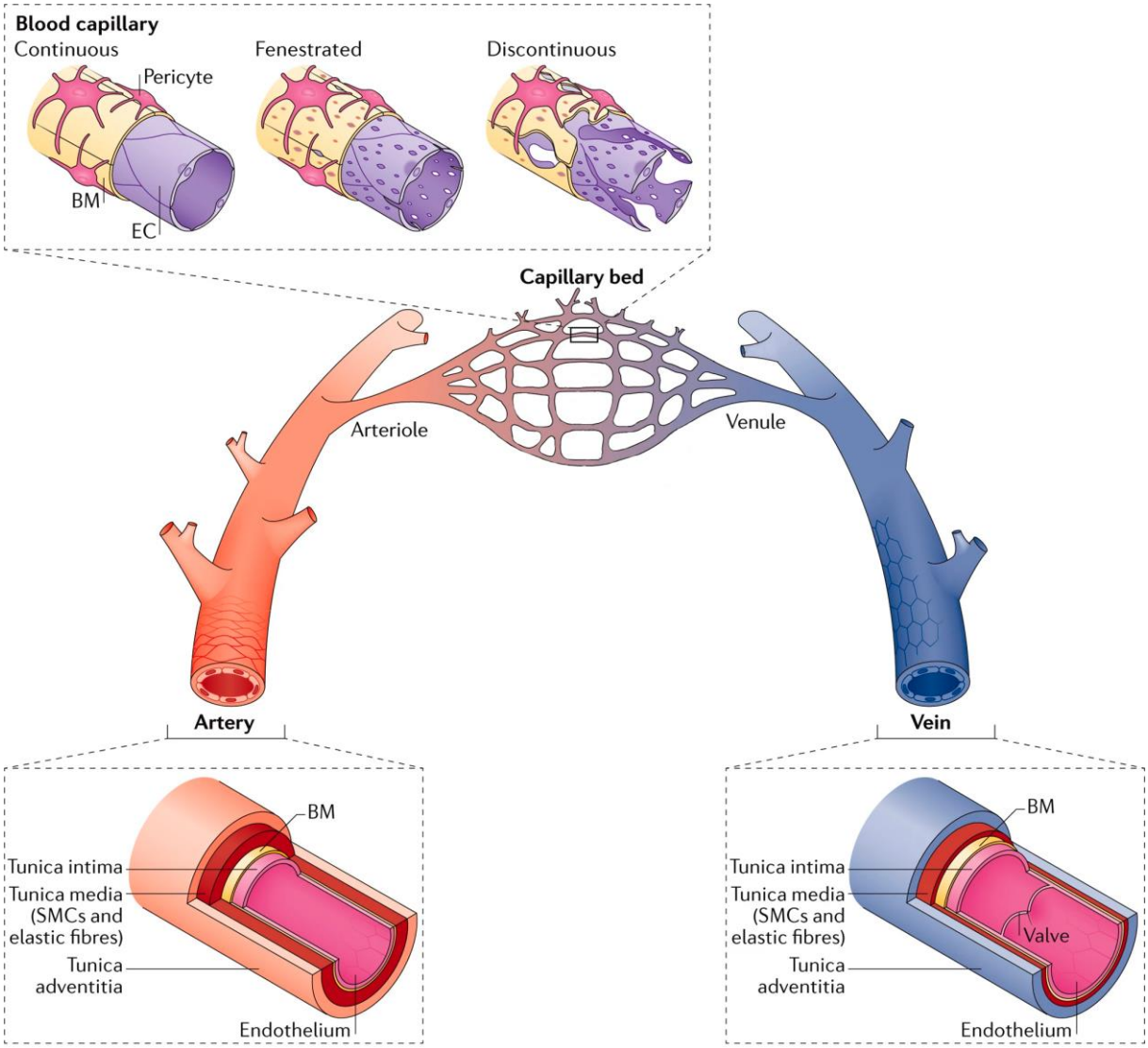

FIGURE 1. The vasculature consists of arteries (red), veins (blue) and interconnected microvasculature that includes arterioles, capillaries and venules. Large arteries and veins have a continuous lining of endothelial cells (ECs), basement membrane (BM) and layers of smooth

muscle cells (SMCs) whereas capillaries can have either continuous, fenestrated or discontinuous lining of ECs and they have a varying amount of BM and pericyte coverage. The anatomy of capillaries is shown at the top of the figure and larger arteries and veins are shown at the bottom. (Adapted from Potente & Mäkinen 2017)

Structural changes in capillaries due to obesity and CMD. Obesity, defined as having a body mass index (BMI) greater than 30 kg/m^2, and its associated metabolic diseases can impair the microcirculation in different organs. These alterations in the capillary network include among other things changes in capillary number and capillary dilation. However, it should be noted that these morphological and functional changes are organ-specific, and the changes seen in one tissue might not happen in another. Whether these changes occur due to angiogenesis or other mechanisms, is still under investigation, although several potential mechanisms have been introduced. (Paavonsalo et al. 2020) Angiogenesis is an event in which new vessels are generated from pre-existing ones through vessel sprouting, branching and anastomosis (Potente & Mäkinen 2017).

3 ANATOMY AND VASCULATURE OF HUMAN AND MOUSE PANCREAS

3.1 Anatomy of human and mouse pancreas

Anatomy. Pancreas is an internal organ that, in humans, is a well-defined solitary organ that can be divided into either three or four anatomical regions: head, neck, body and tail (Figure 2). Some authors may study the head and neck regions as whole, therefore reducing the number of regions to three. However, it should be noted that in reality, none of the anatomical regions have clear-cut borders between each other. The human pancreas weighs around 50–100 g. (Dolenšek, Rupnik & Stožer 2015; Ionescu-Tirgoviste et al. 2015) In mice, the pancreas is not as clearly defined organ as it is in humans. Additionally, the regions differ, and they are as follows: duodenal, splenic and gastric lobe (Figure 2). (Dolenšek, Rupnik & Stožer 2015)

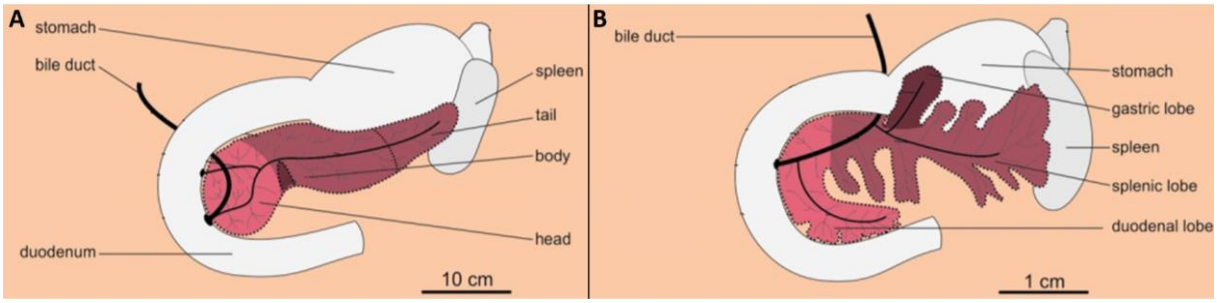

FIGURE 2. Anatomical regions of the human pancreas (A) and mouse pancreas (B) along with their closest internal organs stomach, small intestine and spleen (Adapted from Dolenšek, Rupnik & Stožer 2015).

Both the human and mouse pancreas consist of two structurally and functionally different parts: exocrine and endocrine areas (Figure 3) (Paavonsalo et al. 2020). The majority of the pancreas' mass is composed of exocrine tissue (Paavonsalo et al. 2020), and it includes acinar cells that produce digestive enzymes and a duct that connects the pancreas to the small intestine (Grapin-Botton 2005). The endocrine part of the pancreas consists of islets of Langerhans (pancreatic islets) that are irregular in shape, although mostly circular to oval, and are scattered throughout the exocrine part of the pancreas (Fowler et al. 2018; Rorsman & Ashcroft 2018). Pancreatic islets consist of five cell types: β-cells, α-cells, δ-cells, PP cells and ε-cells. Each cell type is specialized in producing specific hormones, for example, β-cells are specialized in producing insulin and α-cells in glucagon. (Da Silva 2018)

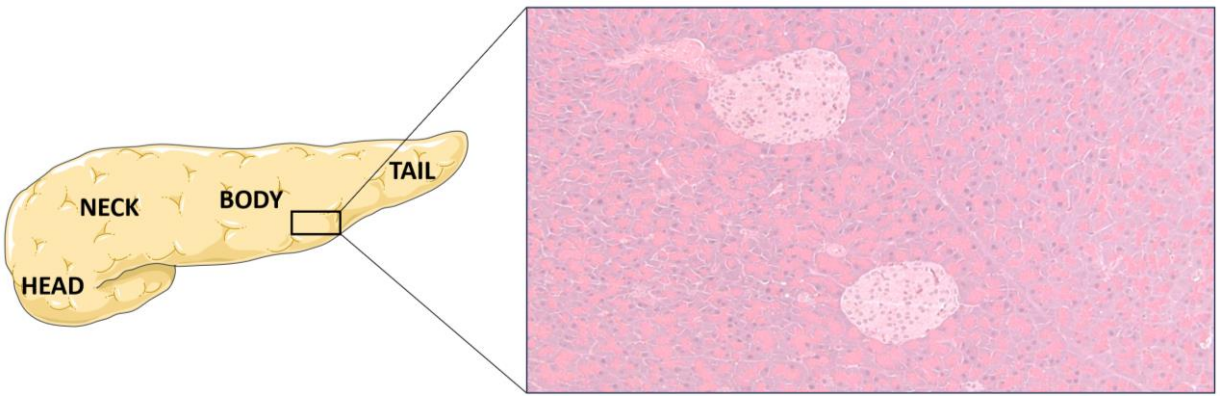

FIGURE 3. An illustration of the anatomical regions of the human pancreas (left) and an example of exocrine (dark pink) and endocrine (lighter pink, round shapes) parts of the mouse pancreas (right) (Adapted partly from picture provided by Servier Medical Art, licensed under Creative Commons Attribution 4.0 Unported License).

Pancreatic islet size. In humans, the diameter of healthy pancreatic islets can seemingly range from 30 μm up to more than 400 μm in diameter (Huang, Harrington & Stehno-Bittel 2018). In a study conducted by Ionescu-Tirgoviste et al. (2015), the average diameter of human pancreatic islets was measured to be around 108 ± 6 μm. Additionally, in the same study, it was shown that the human pancreas seems to "prefer" certain dimensions, as the surface area of over 2/3 of all measured islets was between 1,000 and 10,000 μm^2. According to the authors, if the islets exceeded a surface area of 100,000 μm^2, the islets were observed to be clustered so that several small islets were gathered tightly along larger blood vessels. In rodents, the diameter of pancreatic islets has been shown to range from 20 to 350 μm and the average diameter has been measured to be around 115 μm (Huang, Harrington & Stehno-Bittel 2018). According to Steiner et al. (2010), in mice and rats, the islet size can vary from ten or fewer cells to thousands of cells. Overall, the size distributions of the islets seem to be similar in both humans and mice (Dolenšek, Rupnik & Stožer 2015).

Cellular composition of pancreatic islets. Regarding the cellular composition and architecture of pancreatic islets, there seems to be interspecies differences: in humans, β-cells make up around 50–70 % of all endocrine cells within islets (Cabrera et al. 2006; Dolenšek, Rupnik & Stožer 2015), whereas in mice and rats, the proportion of β-cells is even higher, making up around 70–80 % of all islet endocrine cells (Steiner et al. 2010). According to Steiner et al. (2010) and Brissova et al. (2005), in mice and rats, the β-cells are most often located in the middle of the islets and are surrounded by the other endocrine cell types. In humans however,

according to Brissova et al. (2005), the human islets do not have a similar core–mantle architecture to that of mouse and rat islets but instead, the β-cells are intermingled with α- and δ-cells (Figure 4).

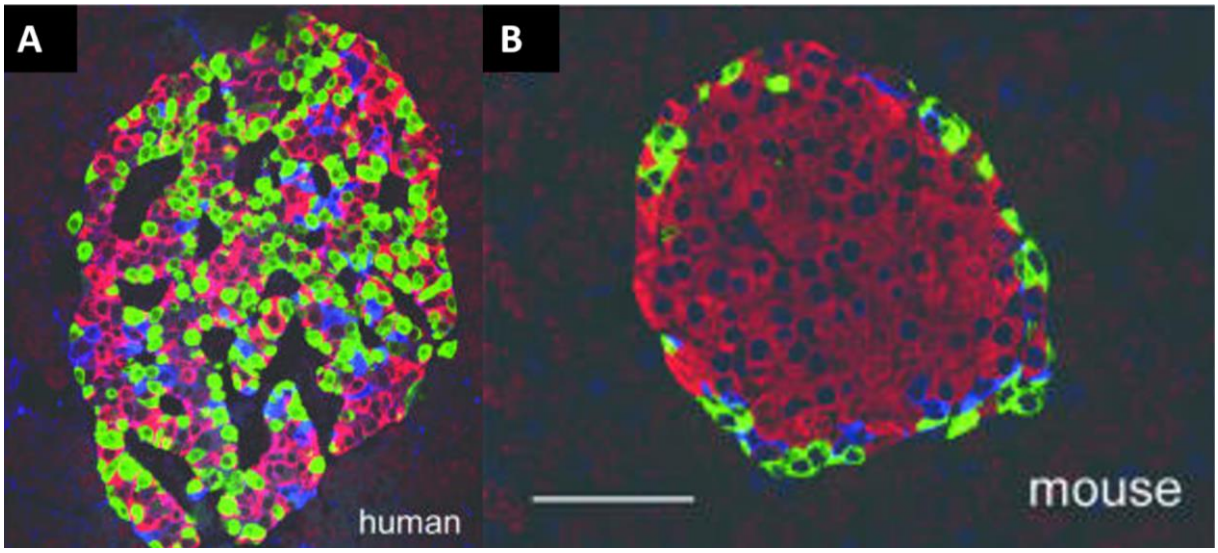

FIGURE 4. Interspecies differences in the islet of Langerhans. An example of a human pancreatic islet (A) and an example of mouse pancreatic islet (B). Insulin-immunoreactive (red), glucagon-immunoreactive (green), and somatostatin-immunoreactive (blue) cells. In this study human pancreatic islets had all three cells randomly distributed throughout the islet of Langerhans whereas in mice, the insulin-containing cells (β-cells) were located in the core of the islet. (Adapted from Cabrera et al. 2006)

Whether the distribution of α-, β- and δ-cells in human pancreatic islets is randomly dispersed throughout the islet or highly structured remains under discussion, however the newer studies are leaning towards a highly structured organization. In an older study conducted by Cabrera et al. (2006), it was concluded that within the islet, α-, β-, and δ-cells had equal and random access to blood vessels and the endocrine cells were not organized in layers around blood vessels. However, in a study conducted by Bosco et al. (2010), it was shown that in human islets, α- and β-cells form a unique arrangement: in small islets (diameter of 40–60 μm), the α-cells were localized in the outer parts and β-cells in the core of the islets, similar to rodent islets. However, in bigger islets (over 60 μm), the α-cells were found also within the islets, always surrounding the blood vessels that were stained with a CD34 antibody. It was also noted that no CD34 staining was observed inside the mass of β-cells. After three-dimensional analysis, the researchers concluded that bigger islets are organized in a trilaminar plate manner: one layer of β-cells

is sandwiched between two α-cell layers and this structure is then folded so that blood vessels circulate along both of its sides (Figure 5). (Bosco et al. 2010) Therefore, although the structure of human islets may initially seem irregular in terms of the organisation of different cell types, it might in fact be a carefully structured complex. However, it should be noted that, according to Steiner et al. (2010), the islet composition can vary within species under different physiological conditions such as diabetes and obesity.

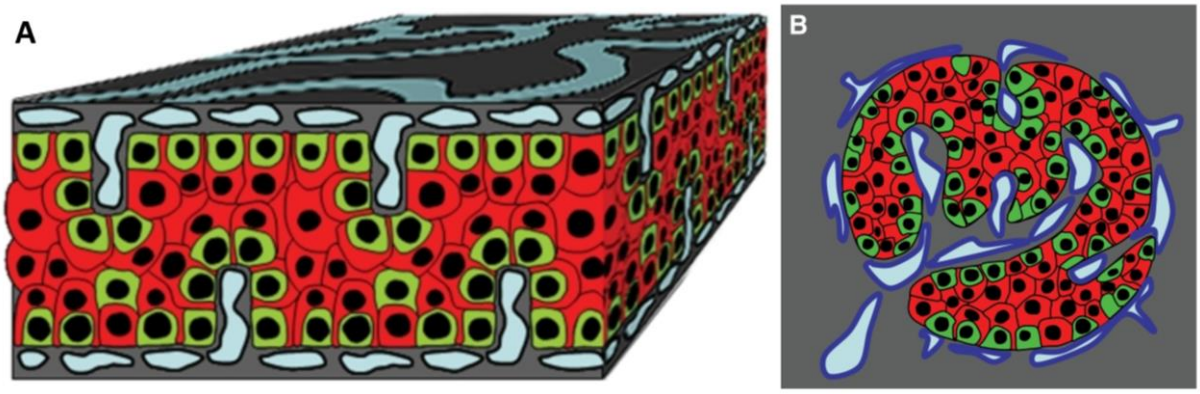

FIGURE 5. A model of a human pancreatic islet and its organization. (A) Vessels (blue) line the both sides of α-cells (green) and β-cells (red) that are organized into a thick folded plate. The α-cells are mostly in the plate's periphery, having a close contact with the vessels. The β-cells are in the more central part of the plate. Most of them develop cytoplasmic extensions that extend between α-cells and therefore reach the surface of the vessels. (B) The plate with adjoining vessels is folded creating an islet. (Adapted from Bosco et al. 2010)

3.2 Vasculature of human and mouse pancreas

Major blood vessels. The anatomy of major arteries and veins is similar in both humans and mice (Dolenšek, Rupnik & Stožer 2015). In the pancreas, the arterial blood is supplied by the abdominal aorta (Dolenšek, Rupnik & Stožer 2015), meaning that the pancreatic islets are exposed to the systemic, and not the portal, glucose concentration (Rorsman & Ashcroft 2018). The abdominal aorta delivers the arterial blood to the pancreas via two major branches: the celiac and the superior mesenteric artery (Figure 6). The celiac trunk (artery) branches into three major arteries: the left gastric, splenic and common hepatic arteries. Of these three, the splenic artery supplies blood to both the body and tail regions of the pancreas whereas the head region is supplied by two arteries originating from the common hepatic artery. The common hepatic

artery is, in fact, first branched into the gastroduodenal artery and then into these two arteries called the anterior and posterior superior pancreaticoduodenal arteries. The venous drainage of the pancreas flows into the hepatic portal vein, and therefore the liver is the first organ to be exposed to pancreatic hormones. (Dolenšek, Rupnik & Stožer 2015; Reynolds et al. 2016)

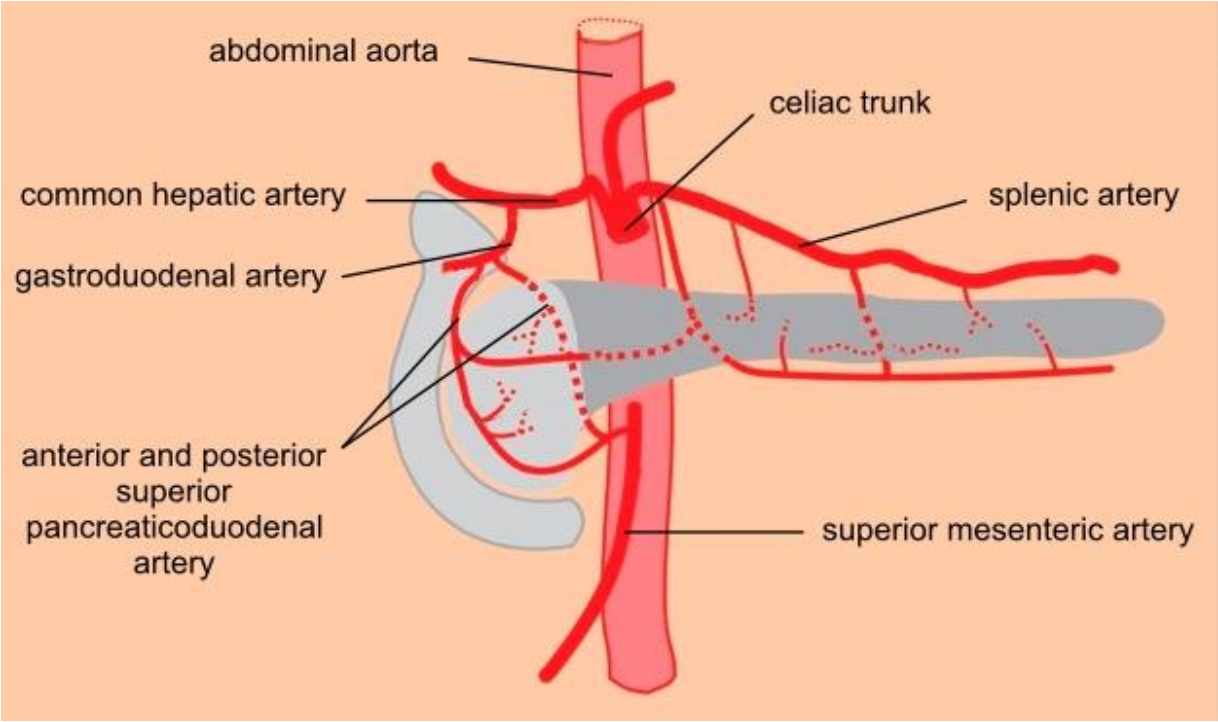

FIGURE 6. Arterial blood supply to the pancreas (Adapted from Dolenšek, Rupnik & Stožer 2015).

Microvasculature. The microvasculature consists of a network of arterioles, venules and capillaries (Dolenšek, Rupnik & Stožer 2015). In pancreatic islets, the blood supply is received from a few feeding arterioles which then branch into a thick network of capillaries (Almaça et al. 2018). In studies using rat models, the microvasculature in pancreatic islets, also called intra-islet capillaries, has been shown to be around five times denser than the capillary network of the exocrine tissue (Jansson & Carlsson 2002; Henderson & Moss 1985). In mice, the density of intra-islet capillaries has been shown to be two times greater than that of exocrine tissue (Brissova et al. 2006). When comparing human and mouse islet capillary densities, a study found that in humans, the islet capillary density was nearly five-fold lower than in mice, and those capillaries were significantly less tortuous (Brissova et al. 2015) (Figure 7). A similar

result was found in a Richardson et al. (2023) study, showing that human islets are less vascularized compared to mouse islets. However, in both species, the capillary density was still greater in the islets compared to the exocrine area.

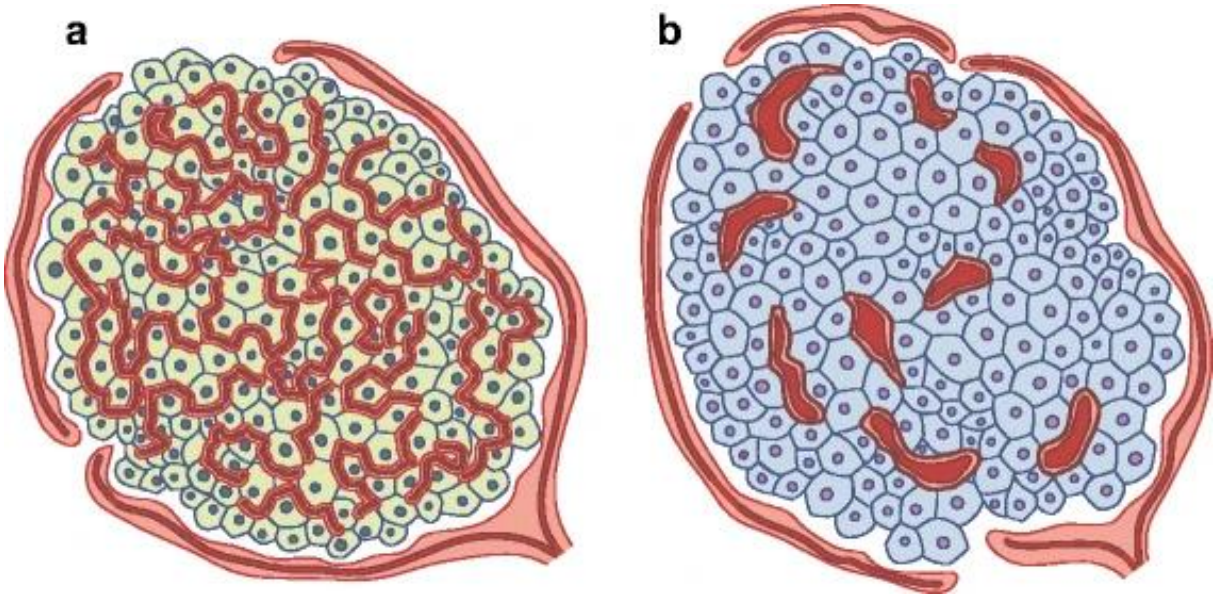

FIGURE 7. An illustration of angioarchitectural differences of (a) rodent and (b) human islets (Hogan & Hull 2017).

The difference in capillary density between human and rodents is not the only distinction between these two species; other notable differences exist as well. In brief, in human islets, the blood vessels contain a greater proportion of smooth muscle cells (Levetan & Pierce 2013) and are surrounded by a double basement membrane (Virtanen et al. 2008). Additionally, the connective tissue layer in perivascular space is denser (Mateus Gonçalves et al. 2020). All in all, it should be noted that in humans, the vascular architecture in the islets is drastically different from that of mice.

Main angioarchitectural differences between endocrine and exocrine tissues. In addition to density differences between endocrine and exocrine tissue, Brissova et al. (2006) highlight other distinctive characteristics between intra-islet and exocrine capillaries. Firstly, although pancreatic islets comprise only around 2 % of the total pancreatic tissue mass, islets can receive up to 20 % of the total pancreatic blood supply (Jansson & Hellerström 1983; Narayanan et al. 2017; Rorsman & Ashcroft 2018), meaning that the islets receive more blood flow than the surrounding exocrine tissue. Secondly, in rodent studies, the islet capillaries have been shown to have a

larger diameter compared to exocrine capillaries (Vetterlein, Pethö & Schmidt 1987; Henderson & Moss 1985; Bonner-Weir & Orci 1982). In Henderson and Moss (1985) study the mean capillary diameter in exocrine capillaries was 4.35 ± 0.3 μm and in endocrine capillaries was 5.27 ± 0.22 μm, whereas in a study conducted by Vetterlein, Pethö & Schmidt (1987), the mean capillary diameter, when all vessels up to 30 μm in diameter were considered, was 5.7 ± 0.2 μm and 6.7 ± 0.2 μm respectively. Thirdly, these intra-islet capillaries have been shown to have up to ten times more fenestrae and thinner walls compared to those of the exocrine capillaries (Henderson & Moss 1985).

4 THE IMPACT OF CARDIOMETABOLIC DISEASE AND EXERCISE ON PANCREATIC VASCULATURE

4.1 The effects of cardiometabolic disease on human pancreas

Pancreas and type 2 diabetes. Type 2 diabetes (T2D) is one of the world's most common metabolic disorders (Galicia-Garcia et al. 2020), and globally it is one of the leading causes of death (World Health Organization 2020). According to a Galicia-Garcia et al. (2020) review, the risk factors of T2D include both genetic and environmental factors. It should be noted that, although the genetics play a role in the development of T2D, T2D can, in many cases, be prevented by improving other main risk factors such as obesity, low physical activity and an unhealthy diet (Galicia-Garcia et al. 2020). In fact, it has been shown that insulin resistance (IR), obesity, and T2D have a close association with one another (Dludla et al. 2023), and in general, most T2D patients are diagnosed as obese or with a higher body fat percentage, especially around the abdominal region (Galicia-Garcia et al. 2020). According to a Dludla et al. (2023) review, the mechanism of T2D pathogenesis is complex.

In the development and progression of T2D, the major pathophysiological derangements are considered to be IR and pancreatic β-cell dysfunction (Dludla et al. 2023). IR refers to a situation where insulin-responsive cells in the liver, muscle and adipose tissues respond insufficiently to insulin (Galicia-Garcia et al. 2020), which then leads to an impaired use and storage of carbohydrates, resulting in a higher blood glucose concentration (Guyton & Hall, 951). To counteract this and to maintain glucose homeostasis, the human pancreatic islets' β-cells increase the production and secretion of insulin (Okajima et al. 2022). Moreover, in addition to increased insulin secretion, studies conducted with obese and overweight nondiabetic individuals have shown a substantial increase (50–90 %) in overall β-cell mass (Figure 8). These compensation strategies are assumed to prevent most obese and insulin resistant individuals from developing T2D. (Chen et al. 2017)

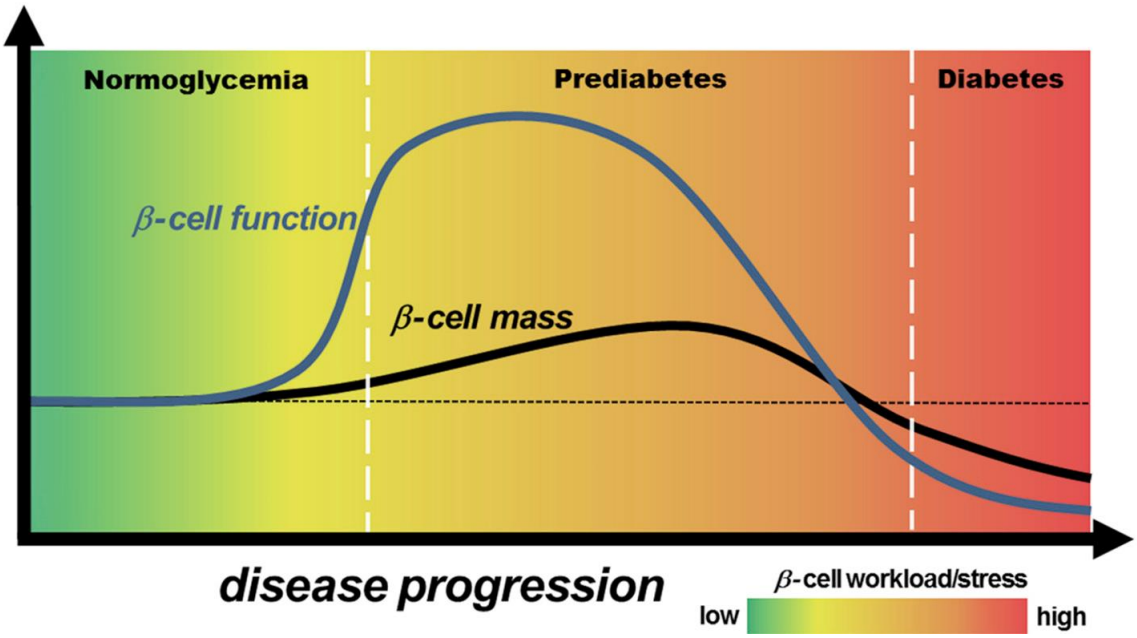

FIGURE 8. Disease progression of type 2 diabetes (Adapted from Chen et al. 2017).

T2D develops when the upregulation of insulin production fails to maintain normoglycemia and β-cell function declines (Okajima et al. 2022) (Figure 8). After the onset of T2D, the insulin secretion capacity has been shown to be reduced by 50–97 % and, the β-cell mass is significantly decreased, even up to 65 % (Chen et al. 2017). In a study by Overi et al. (2022), the composition of pancreatic islets in type 2 diabetic human subjects was shown to have a lower percentage of β-cells (40.2 ± 4.7%) and a higher percentage of α-cells (55.0 ± 9.6%) compared to non-diabetic donors (62.2 ± 4.4% and 31.5 ± 6.1%, respectively). Similar changes in α-/β-cell ratio have also been reported in other human studies (Clark et al. 1988; Butler et al. 2003). This change in α-/β-cell ratio could be due to increased apoptosis (Chen et al. 2021), β-cells losing their differentiated identity, or possibly even gaining features of other islet cell types, as has been described in the reviews by Swisa, Glaser & Dor's (2017) and Chen et al. (2017). Overall, it appears that an impairment of β-cell function is an early feature of disease pathogenesis whereas the substantial decrease in β-cell mass occurs more closely to the clinical manifestation (Chen et al. 2017).

4.2 Effects of type 2 diabetes on pancreatic vasculature

The effects of T2D on pancreatic vasculature have been studied with both human and rodent models. Although the measured variables are often the same, different studies have used slightly different terms or definitions to describe the phenomena. For example, there are some differences in the definition of islet capillary density (ICD): some studies use the definition 'percentage of CD31-positive area relative to the whole islet area' or something similar and others 'the number of capillary particles per islet area' (#/mm^2 or no/mm^2). This difference in definitions does affect the results, and therefore, the used definitions used are mentioned while reviewing the studies. Additionally, as mentioned in the Paavonsalo et al. (2020) review, these definitions might not reflect anatomical capillary rarefaction (number of capillaries/parenchymal cell), as they do not take into account changes in cell size – as increases in cell size will not decrease the number of capillaries per se but will push the capillaries away from each other. It should also be noted that in the most comprehensive studies, researchers include both definitions but under different terms: 'percentage of CD31-positive islet area relative to the whole islet area' refers to capillary area whereas 'the number of capillary particles per islet area' refers to ICD. In the following paragraphs, the studies are described in more detail.

4.2.1 Morphological changes of human pancreatic vasculature in T2D

In a study conducted by Brissova et al. (2015), human autopsy pancreases from nine T2D subjects were used to study capillary density in the pancreas. In this study, ICD was expressed as the number of capillaries per islet area. Compared to the control group, the study showed 36 % greater ICD in subjects with T2D. Additionally, these intra-islet capillaries were thicker and more fragmented compared to the control pancreases. It should be noted that such density change was only seen inside the islets, as the thickness of peri-islet capillaries, vessels that are partly adjacent to endocrine and partly to exocrine tissue, was shown to be similar to that of control islets. Although the ICD increased, the researchers pointed out that an increase in $CD34^+$ capillaries does not necessarily equate to an increase in functional capillaries. They also mentioned that the seeming increase in ICD might be due to vascular thickening that can lead to vessel instability and fragment formation. These changes are then observed as an increased overall vessel count in T2D islets. (Brissova et al. 2015)

In Shah et al. (2016) study, ten autopsy pancreases from T2D subjects were analysed. According to the researchers, the vessel area, defined as CD31/islet area, was shown to be increased compared to non-diabetic controls. However, the study used both terms 'vessel area' and 'vessel density' interchangeably and thus, the overall conclusion was unclear. However, using the same antibody and counting method as Brissova et al. (2015) for ICD, Ling et al. (2020) were able to observe differences in ICD depending on whether the human T2D autopsy samples contained amyloid deposits or not. These islet amyloid deposits are formed when islet amyloid polypeptide (IAPP) proteins misfold and clump together, gradually accumulating between β-cells and islet capillaries. Over time, this accumulation can disrupt the normal function of the pancreas. In the study, both amyloid positive T2D group and amyloid-free T2D group had similar islet area but, in the amyloid-free group, the ICD was significantly higher compared to the group with amyloid deposits. Therefore, it was concluded that amyloid depositions are associated with decreased ICD. (Ling et al. 2020)

In another autopsy study, Takahashi et al. (2021) examined Japanese non-obese T2D and non-diabetic patients who had either died of acute myocardial infarction (AMI) or were free from it. The study used the same definition of ICD as Brissova et al. (2015) and Ling et al. (2020). In this study, diabetic patients who died of AMI had increased ICD compared to the other three groups. Additionally, in both diabetic groups, the vascular basement membrane was thicker compared to the non-diabetic groups. In general, both diabetic and non-diabetic patients who had died of AMI showed an increased capillary area, defined as the percentage of CD31-positive area including their lumens relative to the whole islet area, compared to those who did not die from AMI. Moreover, the non-diabetic patients who had died of AMI showed significantly greater islet capillary size compared to the other three groups. (Takahashi et al. 2021)

Overall, studies conducted with human autopsy samples show both increases and decreases in ICD along with changes in capillary thickness and fragmentation. Collectively, these studies provide evidence of alterations in islet capillary morphology and ICD in T2D (Figure 9) but according to the Takahashi et al. (2021) study, the structural changes of microvasculature seen in pancreatic islets are similar to those seen in the heart, kidney, retina, and peripheral nerve tissues suffering from microangiopathy.

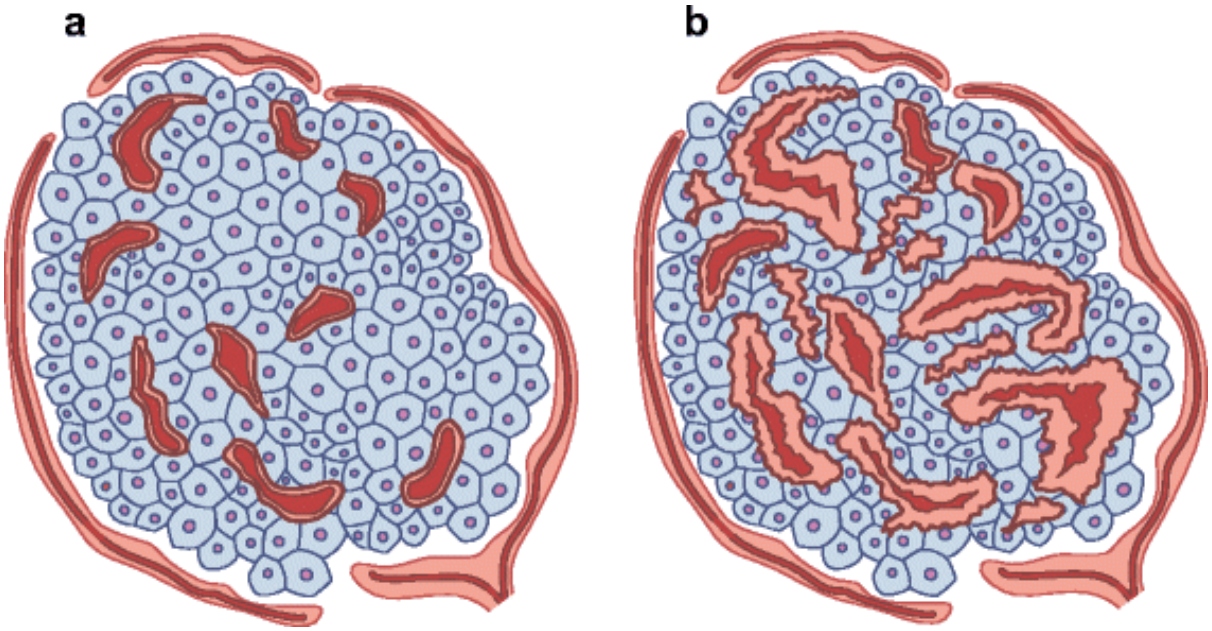

FIGURE 9. An illustration of islet capillary morphology and density between (a) human subjects without T2D and (b) those with T2D. In T2D, intra-islet capillary density is increased, and capillaries seem to be thickened and fragmented. (Hogan & Hull 2017)

4.2.2 Morphological changes of rodent pancreatic vasculature and islet size in insulin resistance and type 2 diabetes

Morphological changes of rodent pancreatic vasculature in IR and T2D have been studied with several rodent models. In all of the following studies conducted with both mice and rats, altered islet capillary morphology has been described. In the following paragraphs, these studies are described in more detail.

Mouse models. Three studies involving db/db mice, a model that is genetically leptin receptor deficient (Burke et al. 2017) and is known to display the key features of human T2D (Burke et al. 2017; Okajima et al. 2022), were found: in the study by Nakamura et al. (1995), islet capillaries of 4-month-old db/db mice were, in general, larger and more diverse in size compared to those of the control mice, and the capillary walls were thicker due to hypertrophied pericytes. Additionally, the ICD, defined as the number of capillary particles per islet area, was significantly decreased as these intra-islet capillaries were less frequently observed. In line with these results, islet capillary diameters of the db/db mice in the Okajima et al. (2022) study were as well significantly increased at 8 and 12 weeks of age, but then suddenly, at 16 weeks of age,

these capillaries contracted. However, these changes in diameters were in line with the changes in islet areas which, similar to the diameters, gradually increased during 4–12 weeks of age, but then declined at 16 weeks of age. Using a similar definition of ICD as Nakamura et al. (1995), Okajima et al. (2022) instead found a significant increase in the number of capillary particles per islet area in db/db mice and the vasculature was found to be meandering. In a third study, Hogan et al. (2017), observed similar enlargement and thickening of intra-islet capillaries in 5-week-old db/db mice backcrossed onto a C57BL/6J background that were studied at 8 or 16 weeks of age. However, in contrast to the two previous studies, ICD was defined as the percentage of CD31-positive islet area and in this case, no significant change was observed. Nonetheless, as mentioned earlier, this definition of ICD is only used in a few studies, and in more comprehensive studies, this definition is used to define capillary area. To conclude, all three studies found enlargement and thickening of intra-islet capillaries, similar to the findings of human samples mentioned earlier, however, the results regarding ICD differed in all three studies.

Two studies involving genetically leptin deficient ob/ob mice (Muzzin et al. 1996) were found (Dai et al. 2013; Okajima et al. 2022). Similar to db/db mice, ob/ob mice become severely obese and hyperglycaemic (Burke et al. 2017; Okajima et al. 2022). In both studies, the islet size was significantly increased, and the islet capillary diameters were progressively increased with age. Additionally, both studies used the same definition of ICD (number of capillary particles per islet area) and both observed a gradual decrease in ICD with age (Dai et al. 2013; Okajima et al. 2022). However, in the Okajima et al. (2022) study, the researchers mentioned that the decrease in ICD only reflected the enlargement of islet size, meaning that the number of capillaries did not decrease in themselves but rather the area containing the capillaries increased. In addition to islet capillaries, Dai et al. (2013) measured the changes in exocrine vasculature but found it unchanged in insulin-resistant ob/ob mice. Furthermore, Dai et al. (2013) examined the islet vascularization with two additional models of IR: 1) male C57BL/6J mice fed with high fat diet (HFD) to induce obesity, and 2) non-obese mice with an inactivated GLUT4 glucose transporter gene. The results were similar to those of ob/ob mice and as such, the researchers concluded that IR leads to an increased capillary area per islet, but it is not due to an increased ICD or angiogenesis but rather that the individual sizes of all capillaries had increased.

A few other studies using transgenic mice were found. In the Agudo et al. (2012) study, C57Bl6/SJL transgenic mice fed with an HFD for 4 months showed an increase in islet size and

vascular thickening together with an increased capillary area-to-islet area ratio. Although the researchers concluded that this alone indicated a higher islet vascularization, it should be argued that an increase in capillary area does not necessarily mean an increase in blood vessel number.

In a newer most comprehensive study focusing on amyloid depositions and T2D, both 2D and 3D analysis techniques were used to study male hemizygous hIAPP transgenic and non-transgenic mice (Castillo et al. 2022). The transgenic mice express the human islet amyloid polypeptide (hIAPP), resulting in amyloid deposits over time. These mice were fed with either an HFD or a low-fat diet (LFD) for around 15 months. Aligning with the previously described studies, this study also observed an increase in mean islet areas in both HFD groups whereas the islet capillary diameter was group dependent such that in the transgenic mice the mean islet capillary diameter was significantly larger in capillaries near to amyloid deposits. Interestingly, using the ICD definition previously described (Dai et al. 2013; Nakamura et al. 1995; Okajima et al. 2022), the changes in ICD were also group dependent: in LFD groups, the ICDs were similar with one another whereas in HFD groups, among non-transgenic mice, the ICD was significantly higher when compared to LFD non-transgenic mice, and in transgenic mice, HFD mice showed no increase in ICD relative to LFD transgenic mice. Comparing the HFD transgenic mice to non-transgenic mice, ICD was significantly decreased in the former, despite similar islet area. Therefore, it was concluded that the changes in ICD and islet capillary diameter were related to amyloid depositions: when the ICD was decreased, it was accompanied by an increased capillary diameter. This finding is in line with the Ling et al. (2020) human autopsy study showing a selective decrease in ICD in areas close to amyloid depositions. This negative effect caused by the amyloid deposits was considered to be caused by vessel fragmentation, rarefaction or cell death. It was also noted that amyloid deposition may inhibit angiogenesis within the islet as the β-cell population expands. (Castillo et al. 2022) With regard to percentage of CD31-positive islet area, no differences were found between the groups (Castillo et al. 2022), showing that the number of capillaries and the percentage of CD31-positive islet area should not be regarded as the same, as was done in the Agudo et al. (2012) and Hogan et al. (2017) studies.

Rat models. Two rat studies concentrating on vascular changes in IR and diabetes have described dilation and/or thickening of islet capillaries together with decreases in ICD (Li et al. 2006; Mizuno et al. 1999). In the Mizuno et al. (1999) study, two groups of 1-year-old Otsuka

Long-Evans Tokushima fatty (OLETF) rats were analysed. In the lean, already severely diabetic group, the islets were degenerated and the number of capillaries in islets was decreased. However, in the obese group where the mice were diabetic but not severely so, the angioarchitecture was similar to that of the control group. In the Li et al. (2006) study conducted with 12-week-old Zucker Diabetic Fatty (ZDF) rats, the rats went through a phase of an islet expansion and later islet failure similar to that observed in humans. The authors also found morphological changes in the microvasculature of the pancreatic islet before the onset of hyperglycaemia, including thickening of capillaries. Additonally, in parallel to islet degeneration, decreases in the ICD were found. In this study, the vasculature was studied with an endothelial cell marker nestin, and the decrease was defined by lower number of nestin positive cells. (Li et al. 2006)

Additionally, in Hayden et al. (2008) human islet amyloid polypeptide (HIP) rat study, transmission electron microscope (TEM) was used to analyse ultrastructural changes in the rats' islet microcirculation. The HIP rat model refers to transgenic rats that develop diabetes between 5 and 10 months of age (Butler et al. 2004). In the 14-month-old rats, TEM showed capillary rarefaction of intra-islet capillaries. Conversely, in the peri-islet capillaries the researchers detected enhanced angiogenesis. (Hayden et al. 2008) However, Paavonsalo et al. (2020) pointed out that the results were only based on visual observations and that no quantifications of capillaries or their density were made.

Summary. In conclusion, these studies show that IR and T2D lead to morphological changes in both human and rodent intra-islet vasculature while the vasculature in the exocrine area remains mostly unaltered (Brissova et al. 2015; Dai et al. 2013). Although most human studies showed an increase in ICD, the findings related to the ICD in rodent models were more varying, influenced by the specific model, the age of the animals, and the definition and measurement method of ICD. However, the majority of rodent studies found consistent morphological changes in terms of enlarged and thickened islet capillaries across different rodent models. These changes were consistent with human studies. Overall, it seems that vascular remodelling in islets happens through the dilation of pre-existing capillaries and not through angiogenesis, therefore compensating for this lack of angiogenesis by increasing thickness and/or dilation. (Agudo et al. 2012; Brissova et al. 2015; Dai et al. 2013; Hogan et al. 2017; Li et al. 2006; Nakamura et al. 1995; Okajima et al. 2022; Takahashi et al. 2021) Altogether, these alterations in vasculature may contribute to the pathophysiology of T2D.

4.3 Impact of exercise on T2D and pancreatic vasculature

The treatment of T2D is based on both lifestyle interventions and medications (Weinberg et al. 2023). With regard to exercise, regular physical activity (PA) from moderate to vigorous intensity, including both aerobic and resistance training, has been shown to have several clinical benefits, such as improved β-cell function, enhanced insulin sensitivity and better blood glucose levels, which result in reductions in glycated haemoglobin (HbA1c) (Amanat et al. 2020; Heiskanen et al. 2018). According to a Thyfault & Bergouignan (2020) review, drug therapies typically only influence either β-cell function or insulin sensitivity whereas exercise enhances them both. Additionally, exercise can also positively affect the lipid profile, blood pressure, and reduce inflammation. Overall, regular exercise is shown to have a positive influence on most of the known T2D factors, reducing the overall risk of developing any cardiovascular diseases. (Amanat et al. 2020; Thyfault & Bergouignan 2020) In the newest consensus statement on exercise and T2D, the term PA was included to give broader definition of human movement, not restricted to only structured or planned exercise, thereby encouraging individuals to reduce sedentary time and include frequent activity breaks between sitting (Kanaley et al. 2022). This statement was an update from the 2010 position stand published by the American College of Sports Medicine (ACSM) and the American Diabetes Association (ADA) (Colberg et al. 2010). In summary, current exercise recommendations for T2D are the same as for healthy individuals, with only a few exceptions and modifications (Kanaley et al. 2022).

With regard to overall morphology of the pancreas, a study conducted with Sprague-Dawley rats (Carvalho et al. 2023) found that after 60 weeks of exercise intervention, the islet morphology of exercised rats was comparable to that of sedentary rats at 26 weeks of exercise intervention, displaying the protective effect of exercise. However, no previous literature on exercise and its effects on pancreatic vasculature in either human or rodent model studies was found during the literature search.

5 RESEARCH QUESTIONS AND HYPOTHESES

The purpose of this thesis was to examine the morphological changes that overweight and exercise (together and separately) cause in the pancreas' vasculature in mice. The main interest was focused on islet capillary density, defined as 1) the number of capillary particles per islet area (no/μm^2) and 2) the number of capillary particles per the number of nuclei in islets. The aim is to increase knowledge about the benefits of exercise on internal organs.

Research question 1: What happens to pancreatic islets (endocrine) and exocrine capillary density in mice in response to obesity and exercise?

Hypothesis: In obesity, there might be significant changes in capillary density of pancreatic islets, but not in the exocrine tissue. The exercise can potentially mitigate these changes in ICD in obesity, while having no visible impact on the capillary density of exocrine tissue.

Rationale: Several rodent studies have reported conflicting results regarding ICD, with findings showing no changes (Castillo et al. 2022; Mizuno et al. 1999), a decrease (Castillo et al. 2022; Dai et al. 2013; Li et al. 2006; Mizuno et al. 1999; Nakamura et al. 1995), or an increase in ICD (Castillo et al. 2022; Okajima et al. 2022) in response to obesity and weight gain. The previous research outcomes seem to be influenced by the specific rodent model used, the age of the animals, and the severity of T2D, as rodents with advanced age or more severe T2D have more often shown a decrease in ICD (Castillo et al. 2022; Dai et al. 2013; Li et a. 2006; Mizuno et al. 1999). Moreover, recent studies focusing on amyloid deposits in both rodents and humans have shown a selective decrease in ICD in areas close to the amyloid deposits (Castillo et al. 2022; Ling et al. 2020). Studies investigating changes in peri-islet and exocrine tissue are scarce; however, their vasculature appears to remain mostly unaltered in both human and rodent models (Brissova et al. 2015; Dai et al. 2013). Studies using the definition of 'the number of capillary particles per islet nuclei' were not found during the literature review. Moreover, no studies on the effect of exercise on pancreatic capillary density were found during the literature search. However, research have shown that exercise can have a protective or even positive effect, reducing the overall risk of developing any cardiovascular diseases (Amanat et al. 2020; Carvalho et al. 2023; Thyfault & Bergouignan 2020).

Research question 2: What happens to capillary area and diameter in pancreatic islets and exocrine tissue of the mouse pancreas in response to overweight and exercise?

Hypothesis: In response to obesity, the capillary area and diameter in pancreatic islets of mice will increase, and exercise could potentially mitigate this effect. In exocrine tissue, no changes will be seen.

Rationale: In general, it seems that the vascular remodelling in pancreatic islets due to obesity and T2D occurs through dilation of pre-existing capillaries and not through angiogenesis, thus compensating for this lack of angiogenesis by increasing thickness and/or dilation. (Agudo et al. 2012; Dai et al. 2013; Hogan et al. 2017; Li et al. 2006; Okajima et al. 2022; Takahashi et al. 2021). In the exocrine vasculature, no changes due to overweight have been detected (Brissova et al. 2015; Dai et al. 2013). The impact of exercise has not been studied. However, as mentioned in the first research question, the exercise can have a protective effect, reducing the overall risk of developing any cardiovascular diseases (Amanat et al. 2020; Carvalho et al. 2023; Thyfault & Bergouignan 2020).

6 METHODS

6.1 Experimental setup

Animals and experimental design. The study was conducted with C57BL/6J adult male mice, which are commonly used in both exercise and metabolic studies. The mice were fed with either a Chow diet or a Western diet (WD, Research Diets D12451), the latter to induce obesity and cardiometabolic diseases (CMD). The mice were randomized into four groups, 10 mice in each: 1) lean sedentary 2) obese sedentary, 3) lean exercise and 4) obese exercise (Figure 10). The WD was started in young adult mice at around eight weeks of age and was continued for 18 weeks. Exercise training for groups 3 and 4 was started at nine weeks after the commencement of WD and it continued until the end of the study.

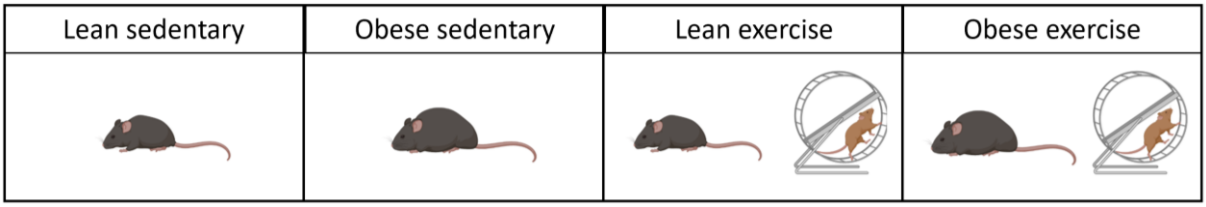

FIGURE 10. Four mouse groups used in the study.

Voluntary running for the exercise groups was enabled by adding running wheels to their home cages. The amount of exercise was recorded automatically. Maximal running tests along with DXA body composition measurements were performed twice during the study: before adding the running wheels (weeks 8 and 9) and in the end of the study (weeks 17 and 18). Additionally, the mice were weighted weekly. Glucose tolerance tests were performed once at the end of the study (around week 17) using intraperitoneal insulin and oral glucose tolerance tests and serum samples were collected before, during, and after the experiment.

Tissue collection and preparation. At the end of the experiment, the mice were euthanized using terminal anesthesia and the tissues (heart, liver, pancreas, white and brown adipose tissue and various skeletal muscles) were collected, weighed and appropriately prepared. The pancreas and left liver lobule were fixed in 4 % paraformaldehyde (PFA) at 4 ℃ for 24 h. The processing, paraffin embedding and cutting of the paraffin-embedded tissues into 5 µm sections with a cryostat were done at NOVA hospital molecular pathology lab in Jyväskylä.

Ethics statement. All animal experimental procedures were in accordance with the European Communities Council Directive (86/609/EEC), and ethical issues were discussed in terms of the "three R's". The animal protocols were approved by the National Animal Experiment Board (ESAVI/22658/2018). All research activities followed good scientific and clinical practices according to the updated guidelines of the National Advisory Board on Research Integrity in Finland.

6.2 Haematoxylin-eosin staining

The haematoxylin-eosin (H&E) protocol consisted of four main steps: deparaffinization, staining, dehydration and mounting. During deparaffinization, the paraffin was removed using xylene and a series of decreasing ethanol solutions. The final solution was MilliQ water. To stain the negatively charged nuclei, the sections were immersed in haematoxylin for 3 minutes, followed by 10 minutes rinsing with tap water. Afterward, the positively charged cytoplasm was stained by immersing the sections into eosin for 40 seconds. The dehydration was done using increasing ethanol content and finally, xylene. The sections were mounted with xylene based Pertex. The exact staining protocol can be seen in Appendix 1.

6.3 Immunofluorescence staining for paraffin embedded sections

Immunohistochemical analysis is used to mark specific cellular sites with antibodies. Immunofluorescence, one of the immunohistochemistry techniques, uses fluorophore conjugated antibodies to visualize the location of the antibodies. In this study, two antibodies were used: 1) primary antibodies that attach to specific cellular sites, and 2) fluorescence labeled secondary antibodies that attach to certain animal antigens it has been made against to.

6.3.2 Original protocol

For paraffin embedded sections, the staining protocol included the following main steps: deparaffinization, antigen retrieval, blocking, primary and secondary antibody incubation, mounting and imaging. The original protocol was as follows:

Deparaffinization. Tissue sections were washed 3x5 minutes with xylene, 2x5 minutes with 99,5 % ethanol, 2x5 minutes with 96 % ethanol, 5 minutes with 70 % ethanol and 5 minutes with milliQ water.

Antigen retrieval. The sections were boiled in a high pH (9.0) Tris EDTA buffer for 20 minutes at 90℃ and then cooled on ice for 20 minutes. Finally, the sections were washed 2x5 minutes with Phosphate Buffer Saline (PBS).

Blocking and primary antibody incubation. For blocking, the sections were incubated at room temperature for 1 hour with 2.5 % normal donkey serum and 0.2 % bovine serum albumin diluted into PBS. Sections were then incubated with primary antibodies overnight in a humified chamber at 4℃. The antibodies and the detailed dilution procedure are presented in Table 1.

TABLE 1. A summary of the primary antibodies and their respective dilutions in the blocking solution.

Tissue	Target	Name	Species	Manufacturer	Cat #	Dilution
Pancreas 1	Blood vessels	Podocalyxin	Goat	R&D Systems	AF1556	1:400
	β-cells	Insulin	Guinea pig	Dako	IR002	no dilution
	Leucocytes	CD45	Rabbit	Abcam	ab10558	1:400
Pancreas 2	Lipid droplets	Perilipin	Guinea pig	Fitzgerald	20R-PP004	1:3000
	Macrophages	F4/80	Rat	Bio-Rad	MCA497R	1:500
Liver	Blood vessels	Podocalyxin	Goat	R&D Systems	AF1556	1:400
	Lipid droplets	Perilipin	Guinea pig	Fitzgerald	20R-PP004	1:3000
	Leucocytes	CD45	Rabbit	Abcam	ab10558	1:400

Secondary antibody incubation and DAPI. After the overnight incubation, the sections were washed for 20 minutes in Tris-NaCl-Tween (TNT) buffer. Immediately after the TNT wash, the sections were incubated with secondary antibodies diluted into PBS Tween (0,05 %

Tween20 in PBS) solution for 1 hour in room temperature in the dark. The secondary antibodies are listed on the Table 2. After the incubation, the sections were washed for 20 minutes with TNT buffer and 2x5 minutes with PBS. DAPI (4′,6-diamidino-2-phenylindole), used as a nuclear counterstain, was added to the section for 5 minutes, after which the sections were washed 2x5 minutes with PBS.

TABLE 2. A summary of secondary antibodies and their respective dilutions in the PBS Tween.

Tissue	Host & Target	Conjugate	Manufacturer	Cat #	Dilution
Pancreas 1	Donkey-anti-goat IgG	Alexa Fluor 555	Invitrogen	A21432	1:500
	Goat-anti-guinea pig IgG	Alexa Fluor 488	Invitrogen	A11073	1:500
	Goat-anti-rabbit IgG	Alexa Fluor 647	Invitrogen	A21245	1:500
Pancreas 2	Donkey-anti-guinea pig IgG	DyLight 549	Not known	Not known	1:500
	Donkey-anti-rat IgG	Alexa Fluor 488	Invitrogen	A21208	1:500
Liver	Donkey-anti-goat IgG	Alexa Fluor 555	Invitrogen	A21432	1:500
	Donkey-anti- guinea pig IgG	DyLight 549	Not known	Not known	1:500
	Goat-anti-rabbit IgG	Alexa Fluor 647	Invitrogen	A21245	1:500

Post-fixation and mounting. The sections were post-fixed with 1 % PFA in PBS for 5 minutes. The sections were washed 2x5 minutes with PBS and 5 minutes with milliQ water. The sections were air dried and mounted using ProLong Diamond antifade reagent.

6.3.3 Protocol adjustment and final protocol

After the initial test staining, inflammation and lipid composition markers were excluded and the following tests focused only on optimizing the blood vessel and β-cell markers of the protocol. For the subsequent test, the β-cell marker was switched to other manufacturer's (Abcam) product and blood vessels were tested also with the isolectin B4 (Vector laboratories) marker. In addition, the secondary antibodies were diluted in PBS instead of PBS-Tween to reduce dissolution of the PAP pen, post-fixation was excluded as an unnecessary step, and the mounting was done on moist samples instead of air-dried ones with Prolong Gold + DAPI antifade reagent.

To optimize the protocol further, the antigen retrieval was first shortened to 10 minutes to diminish epitope spreading, but later lengthened to 15 minutes. Moreover, to block endogenous peroxidase activity and therefore reduce non-specific background, the samples were incubated in 0,3 % H_2O_2 for 30 minutes before blocking. Additionally, the dilution of isolectin B4 was increased from 1:50 to 1:200 and the primary antibody incubation was shortened from overnight at 4℃ to 2 hours at room temperature. To get sharper outlines of nuclei, the mounting medium was switched back to ProLong Diamond and DAPI was added separately. For the assumed final staining, the pancreas blood vessels were stained with isolectin B4 (Vector laboratories) and the β-cells with insulin (Abcam). For liver, podocalyxin (R&D Systems) was used to stain blood vessels.

To our surprise, isolectin B4 did not stain anything inside the β-cells mass (see results). To study this further, the pancreas was first stained with lectin UEA1 (Vector laboratories) and podocalyxin (R&D Systems), and again with isolectin B4 (Vector laboratories), lectin UEA1 (Vector laboratories) and podocalyxin (R&D Systems) to see if any of these markers overlap with one another. Additionally, the protocol was further simplified by reducing the amount of PBS washing steps and replacing TNT buffer with PBS. Moreover, the temperature in antigen retrieval was made sure to go up to 95℃. Based on these results, the final protocol for the pancreas was developed with podocalyxin (R&D Systems) and insulin (Abcam) and for the liver with podocalyxin (R&D Systems). The final protocol was as follows:

Deparaffinization. Tissue sections were washed 3x5 minutes with xylene, 2x5 minutes with 99,5 % ethanol, 2x5 minutes with 96 % ethanol, 5 minutes with 70 % ethanol and 5 minutes with milliQ water.

Antigen retrieval. The sections were boiled in a high pH (9.0) Tris-EDTA buffer for 15 minutes at 95℃ and cooled down on ice for 20 minutes. After this, the sections were washed 2x5 minutes with PBS and the autofluorescence of the sections was removed by incubating the samples in 0.3 % H_2O_2 in PBS for 30 minutes.

Blocking and primary antibody incubation. For blocking, the sections were incubated at room temperature for 1 hour with 2.5 % normal donkey serum and 0.2 % bovine serum albumin diluted into PBS. The sections were then incubated with primary antibodies for 1 hour at room temperature. The antibodies and the detailed dilution procedure are presented on Table 3.

TABLE 3. A summary of the primary antibodies and their respective dilutions in the blocking solution.

Tissue	Target	Name	Species	Manufacturer	Cat #	Dilution
Pancreas 1	Blood vessels	Podocalyxin	Goat	R&D Systems	AF1556	1:400
	β-cells	Insulin	Rabbit	Abcam	ab181547	1:10 000
Liver	Blood vessels	Podocalyxin	Goat	R&D Systems	AF1556	1:400

Secondary antibody incubation. After primary antibody incubation, the sections were washed 3x5 minutes with PBS. Immediately after, the sections were incubated with secondary antibodies diluted in PBS for 1 hour at room temperature in the dark. The secondary antibodies are listed in Table 4.

TABLE 4. A summary of secondary antibodies and their respective dilutions in the PBS.

Tissue	Host & Target	Conjugate	Manufacturer	Cat #	Dilution
Pancreas	Donkey-anti-goat IgG	Alexa Fluor 555	Invitrogen	A21432	1:500
	Donkey-anti-rabbit IgG	Alexa Fluor 488	Invitrogen	A21206	1:500
	UEA1	DyLight 649	Vector laboratories	DL-1068-1	1:200
Liver	Donkey-anti-goat IgG	Alexa Fluor 555	Invitrogen	A21432	1:500

DAPI and mounting. After the incubation, the sections were washed for 5 minutes with PBS, DAPI was added for 5 minutes, and then the sections were washed for 5 minutes with PBS. The sections were mounted using ProLong Diamond antifade reagent.

Negative controls. Negative controls were performed during every staining by using only secondary antibodies and DAPI.

6.4 Microscopy

Haematoxylin-eosin staining. Images were obtained with an Olympus BX50 fluorescence microscope and a 20x objective. The image acquisition parameters were adjusted individually for each image.

Immunohistochemistry. From each sample, five images showing at least one islet of Langerhans were taken. Images were obtained with a Zeiss LSM 700 confocal microscope and a 20x objective. The image acquisition parameters were adjusted individually for each image to achieve optimal intensity and contrast while avoiding over- and underexposed areas. Pancreas and liver samples were observed under the microscope within 24 and 48 hours, respectively, after mounting.

6.5 Image processing and analysis with Fiji/ImageJ

Haematoxylin-eosin images were used as-is, with no further processing, whereas all immunohistochemistry images were further processed with Fiji/ImageJ V2.15.1 software (Schindelin et al. 2012). To reduce variability during image processing and analysis, the processing and analysis were both performed with the ImageJ Macro (IJM) scripting language (see the whole script in Appendix 3). Briefly, the script consisted of three main processes: 1) segmentation of the islets of Langerhans and exocrine area, 2) segmenting the structures of interest, namely the nuclei and the capillaries, and 3) measurement of the desired variables from both the islets of Langerhans and exocrine area. There were four variables measured from both the islets and exocrine tissue: 1) *capillary density* defined as the number of capillaries per selected tissue area (no/μm^2), 2) additional capillary density, *capillaries-to-nuclei ratio*, defined as the number of capillaries per the number of nuclei in selected tissue (capillaries/nuclei), 3) *capillary area* defined as the capillaries' total area per selected tissue area (μm^2/ μm^2), and 4) *Feret's diameter* of capillaries in selected tissue (μm). Feret's diameter was used to indicate of the enlargement of capillaries. For the first two variables, the script used a similar approach to that previously described in studies by Brissova et al. (2015), Castillo et al. (2022), Dai et al. (2013) and Takahashi et al. (2021).

6.6 Statistical analysis

All statistical analyses were performed using GraphPad Prism 10.2.3. Before any statistical analyses, outliers from each variable were systematically identified by calculating the mean and standard deviation for each mouse group and then removing the values that either exceeded the

threshold of ‘mean + 2 x standard deviation’ or fell below the threshold of ‘mean – 2 x standard deviation”. Data points identified as outliers, based on the criteria outlined above, were excluded from further analysis. After the removal of outliers, the mean values for each mouse were recalculated using the remaining data points. The newly calculated mean values for each mouse were then utilized in the final analysis. This should reduce variation due to technical errors in staining or automated data analysis.

Normality was assessed using the Shapiro-Wilk test. Differences between pre- and post results were assessed using a paired t-test. A one-way Analysis of Variance (ANOVA), followed by Fisher's LSD test, was applied to compare the various mouse groups, while an unpaired t-test was employed to compare islet and exocrine tissues. Correlation significance levels were set at $P<0.05$. The results are presented as mean ± SD. All comparisons were performed across all groups.

7 RESULTS

7.1 General physiological outcomes of the nutrition and exercise intervention

Two mice were removed from the exercise groups due to minimal running on running wheels. In this section, the figures illustrate the outcomes of the nutrition and exercise intervention related to maximal running, bodyweight, body composition, and glucose tolerance. In the first test, maximal running, the distance run by the exercising mouse groups was shown to increase in the lean exercise group (p=0,0881) and significantly in the obese exercise group (p=0.0044), whereas in the sedentary groups, the running distances remained relatively the same (Figure 11).

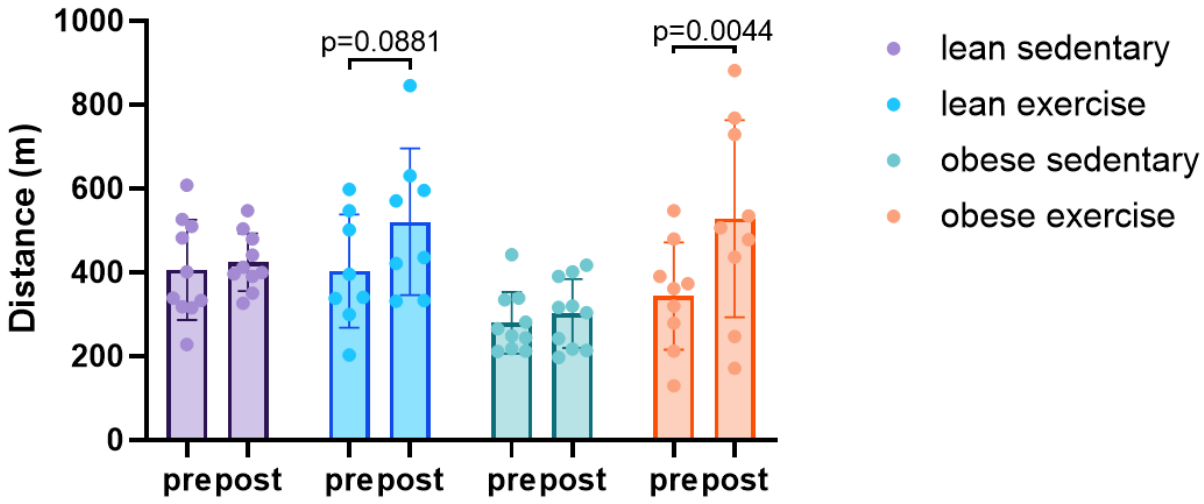

FIGURE 11. Maximal running test. The running distances ran by the different mouse groups during week 9 (pre) right before adding running wheels into home cages and week 18 (post), before the end of the experiment.

Figure 12 illustrates the changes in bodyweight during the intervention across different groups. During the first 9 weeks, the bodyweight increased in all mouse groups, more so in the obese groups. After adding the running wheels, the bodyweight in the exercise groups was shown to be lower compared to the respective sedentary groups. Additionally, Figure 13 shows how the bodyweight increases significantly from week 9 to week 18 in the sedentary groups (lean sedentary p=0.0028, and obese sedentary p=0.0137), whereas in the exercise groups the bodyweight remained around the same level.

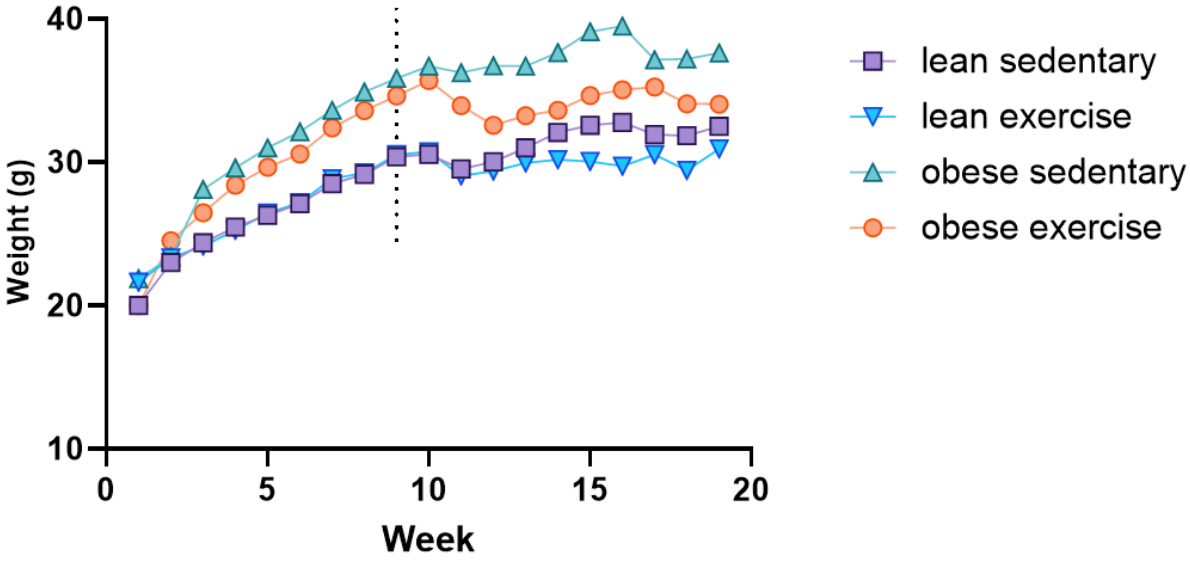

FIGURE 12. Bodyweight measurements from week 1 to week 18. Dash line represents week 9 when the running wheels were added.

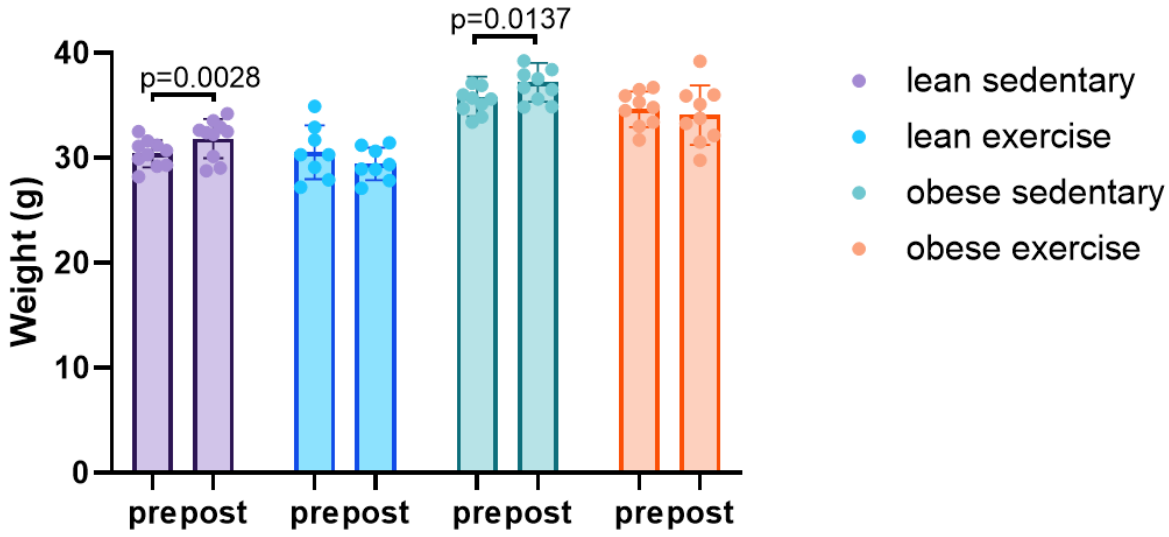

FIGURE 13. Bodyweight on week 9 (pre) right before adding running wheels and week 18 (post), before the end of the experiment. In the sedentary groups, body weight increased significantly (lean sedentary p=0.0028, and obese sedentary p=0.0137) throughout the intervention.

DXA body composition measurements were performed twice during the study: before adding the running wheels and at the end of the intervention. The fat percentages in the obese groups were significantly higher compared to the lean groups ($p<0.0001$), both before and after the exercise intervention (Figure 14). However, in the obese groups, DXA% fat was significantly

lower in the obese exercise group compared to obese sedentary (p=0.0107) after the exercise intervention.

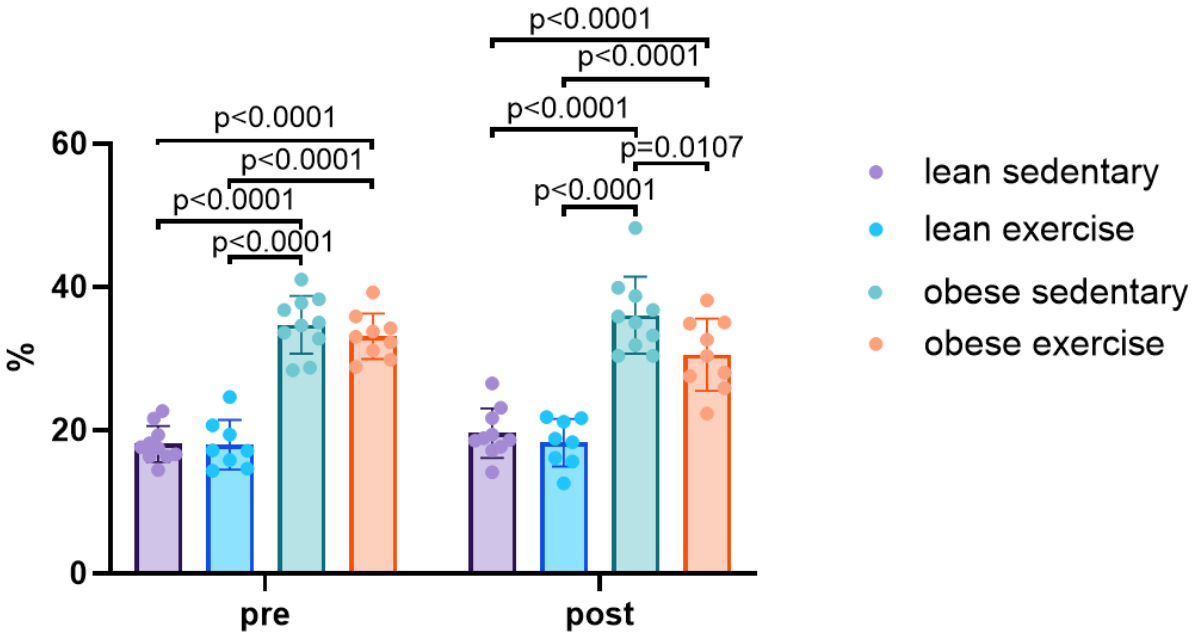

FIGURE 14. Body composition of all mouse groups with DXA% fat measured before adding the running wheels at weeks 8 and 9 (pre) and at the end of the study at weeks 17 and 18 (post).

Glucose tolerance test (GTT) was performed once at the end of the study. In the obese exercise group, GTT results were close to those of the lean groups whereas in the obese sedentary group, blood glucose remained elevated even after 120 minutes (Figure 15). In Figure 16, the area under the curve GTT (AUC GTT) shows that the obese sedentary group has significantly higher values compared to the other groups (p=0.0003, p=0.0001, p<0.0001) and the obese exercise group is close to the values of the lean groups.

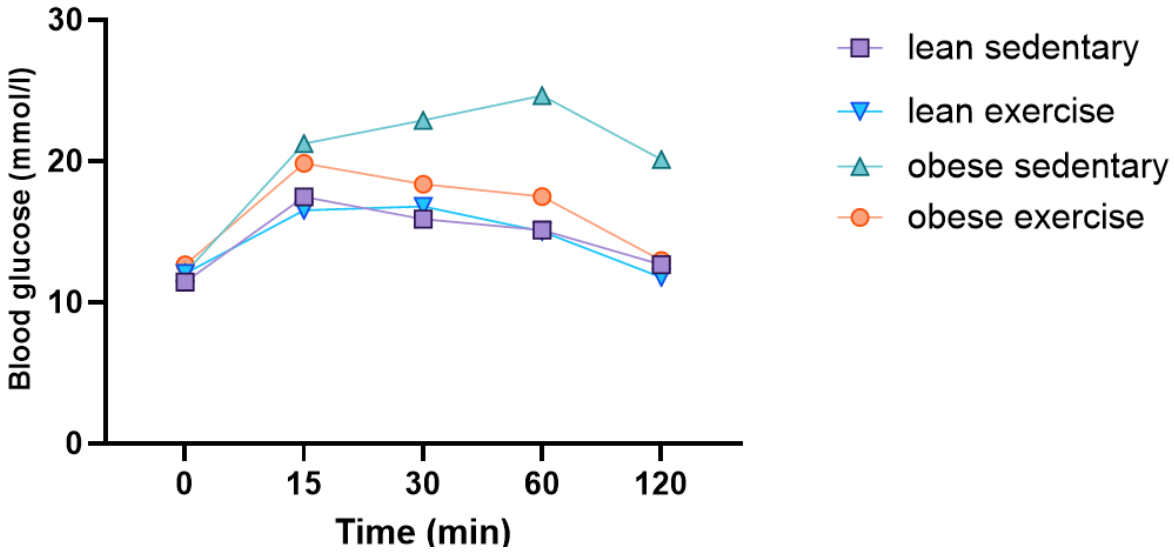

FIGURE 15. Glucose tolerance test (GTT) was performed at the end of the study. The obese sedentary group had higher blood glucose values throughout the 120 minutes period than the other groups.

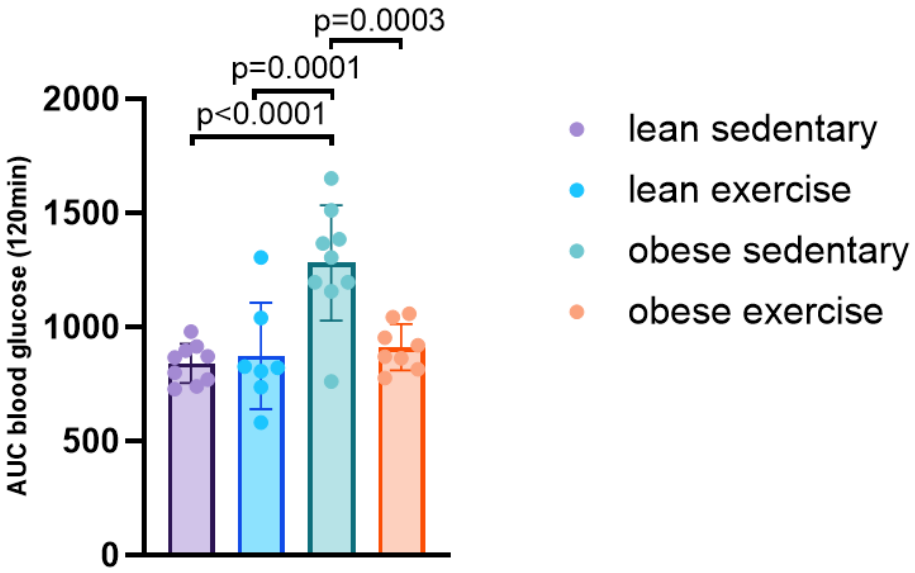

FIGURE 16. Area under the curve in the glucose tolerance test (AUC GTT). The obese sedentary group had a significantly larger AUC compared to the rest of the groups (p=0.0003, p=0.0001, p<0.0001).

7.2 Visual analysis of haematoxylin-eosin-stained pancreas and liver tissues

No image analysis tools were used to measure H&E-stained sections. Therefore, the results discussed here are only based on visual observations. In this section, liver tissue is also discussed as it was both stained and imaged together with pancreas tissue.

In the pancreas sections, no visible differences between the mouse groups were observed (Figure 17). However, in liver sections, there was a difference between the lean and obese groups as the liver sections of obese groups had visibly more often round shaped non-stained (white) areas (Figure 17), which are accumulated lipid droplets. Additionally, there was a clear difference between the obese sedentary and obese exercise group as these round shaped, non-stained areas were observed to be both more frequent and larger in size in the obese sedentary group compared to the obese exercise group. In the obese sedentary, 7 out of 10 mice had visible changes in their liver section whereas in the obese exercise, only 3 out of 10 mice had clear visible changes in the structure. The figures shown below are representative images of each group.

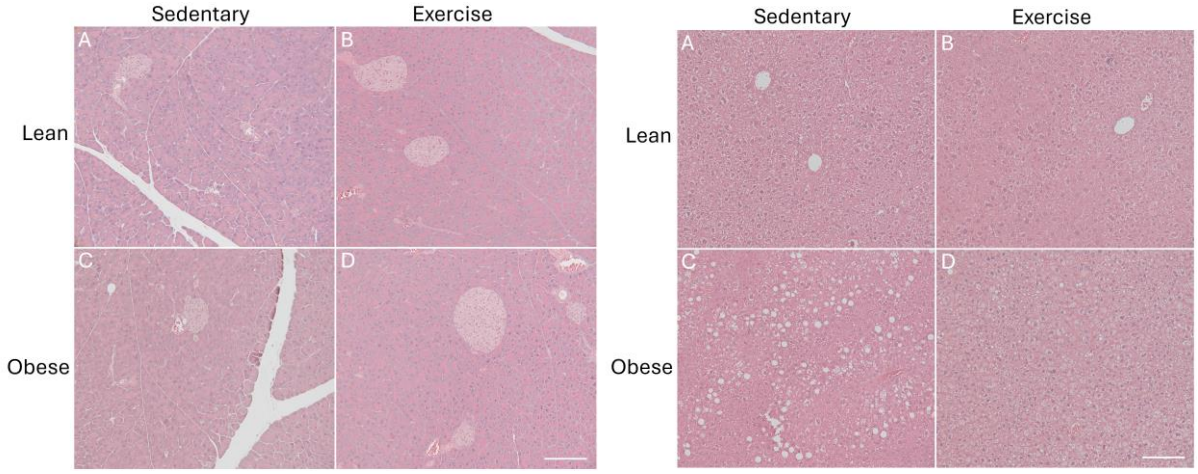

FIGURE 17. Haematoxylin-eosin staining of pancreas (left A–D) and liver (right A–D) sections. In the pancreas sections, the islets of Langerhans are generally oval shaped and slightly lighter in colour. Large white stretch marks seen in images A–C are due to tissue processing. In the liver sections, obese sedentary group had round-shaped, non-stained (white) areas more frequently observed compared to other mouse groups. Scale bar = 100 μm.

7.3 Characterizing capillary changes in immunofluorescence-stained pancreas tissue

7.3.1 Results of the protocol adjustment

In the intended final staining procedure, isolectin B4 (Vector Laboratories) was used to stain the pancreatic blood vessels and insulin antibody (Abcam) was used to stain the β-cells. However, unexpectedly, isolectin B4 failed to stain anything within the β-cell mass, resulting in visibly unstained black areas where the β-cell clusters were located (Figure 18).

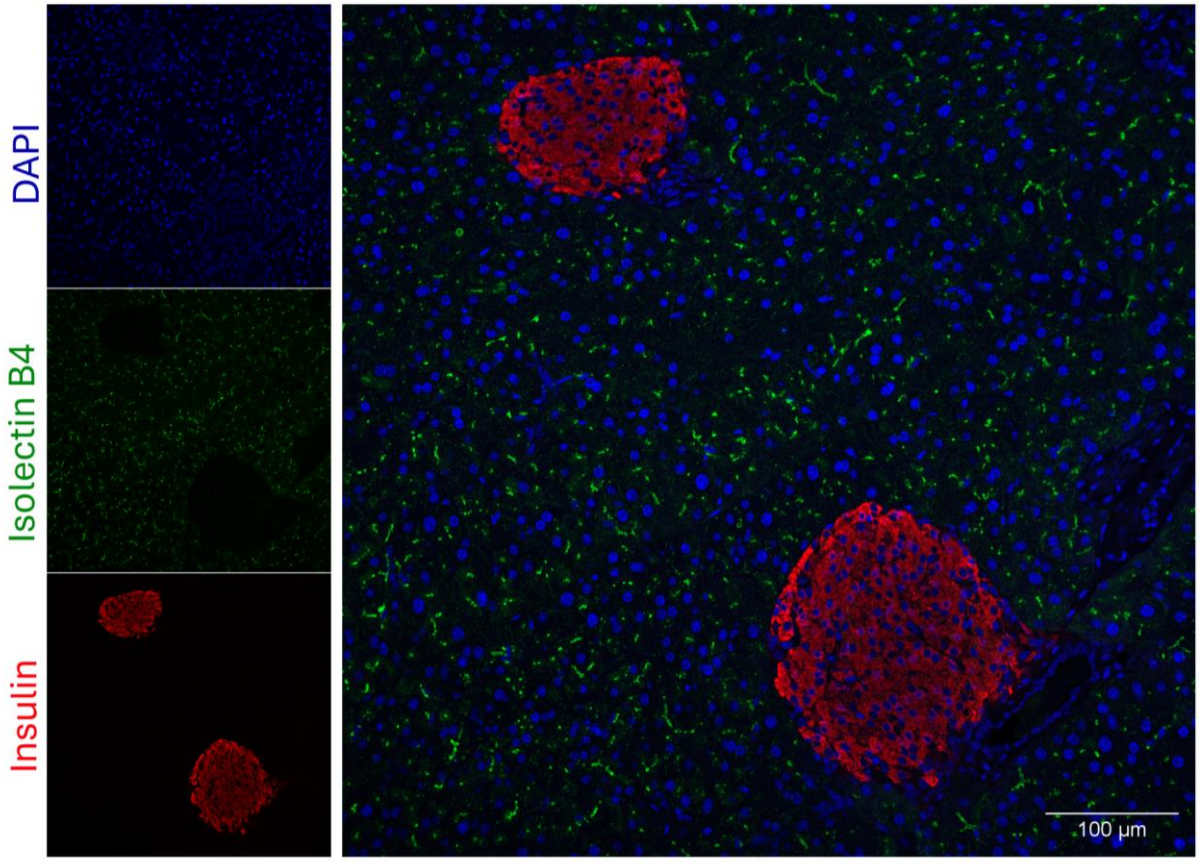

FIGURE 18. Pancreas stained with DAPI (blue), insulin antibody (red) and isolectin B4 (green). Within the insulin-stained area, no isolectin B4 can be detected. Scale bar = 100 µm.

To study this further, the pancreas was first stained with lectin UEA1 (Vector laboratories) and podocalyxin (R&D Systems). Here, lectin UEA 1 did not stain the inside of the β-cell mass, just as the isolectin B4 did not (figure not shown here). Additionally, lectin UEA 1 and podocalyxin did not overlap, bringing up the question “What do these markers really stain in the pancreas?”. Thus, the pancreas was again stained with the following three staining markers: isolectin B4 (Vector laboratories), lectin UEA1 (Vector laboratories) and podocalyxin (R&D

Systems) to see which of these markers overlap with one another. As a result, we could see that 1) neither lectin UEA1 or isolectin B4 stains the inside of the β-cell mass, 2) lectin UEA1 and isolectin B4 partly overlap with one another, 3) podocalyxin does not overlap with either of them, 4) podocalyxin does stain the inside of the β-cell mass (Figure 19).

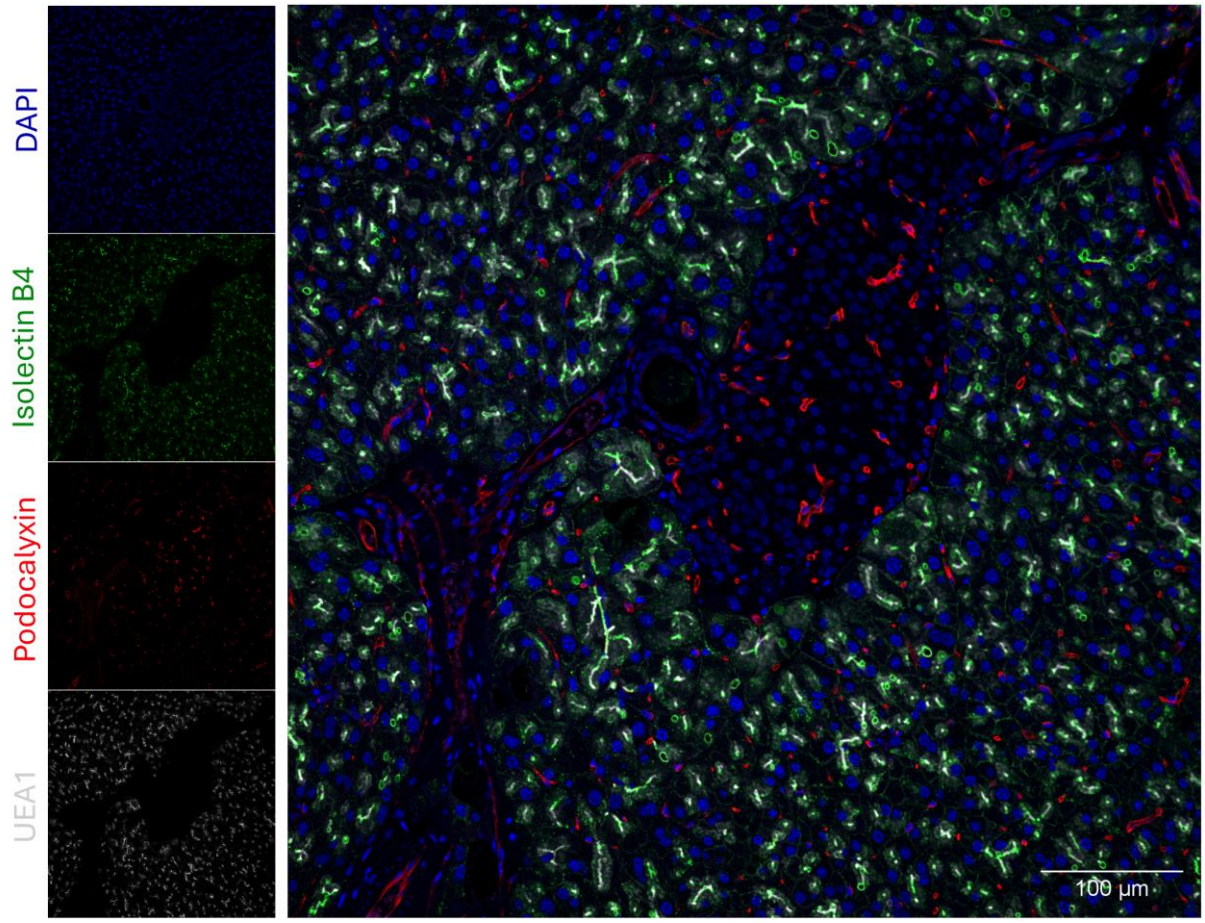

FIGURE 19. Pancreas tissue stained with DAPI (blue), isolectin B4 (green), podocalyxin (red), and lectin UEA1 (white/grey). Of the three of the said blood vessel markers, only podocalyxin was detected inside the β-cell mass. Scale bar = 100 µm.

In addition to the pancreas section, we also applied the same staining procedure described above to a liver section (Figure 20). For the liver, it was shown that 1) lectin UEA1 did not stain anything inside the liver, 2) isolectin B4 was detected but only after overexposure, and 3) podocalyxin stained the liver vasculature well.

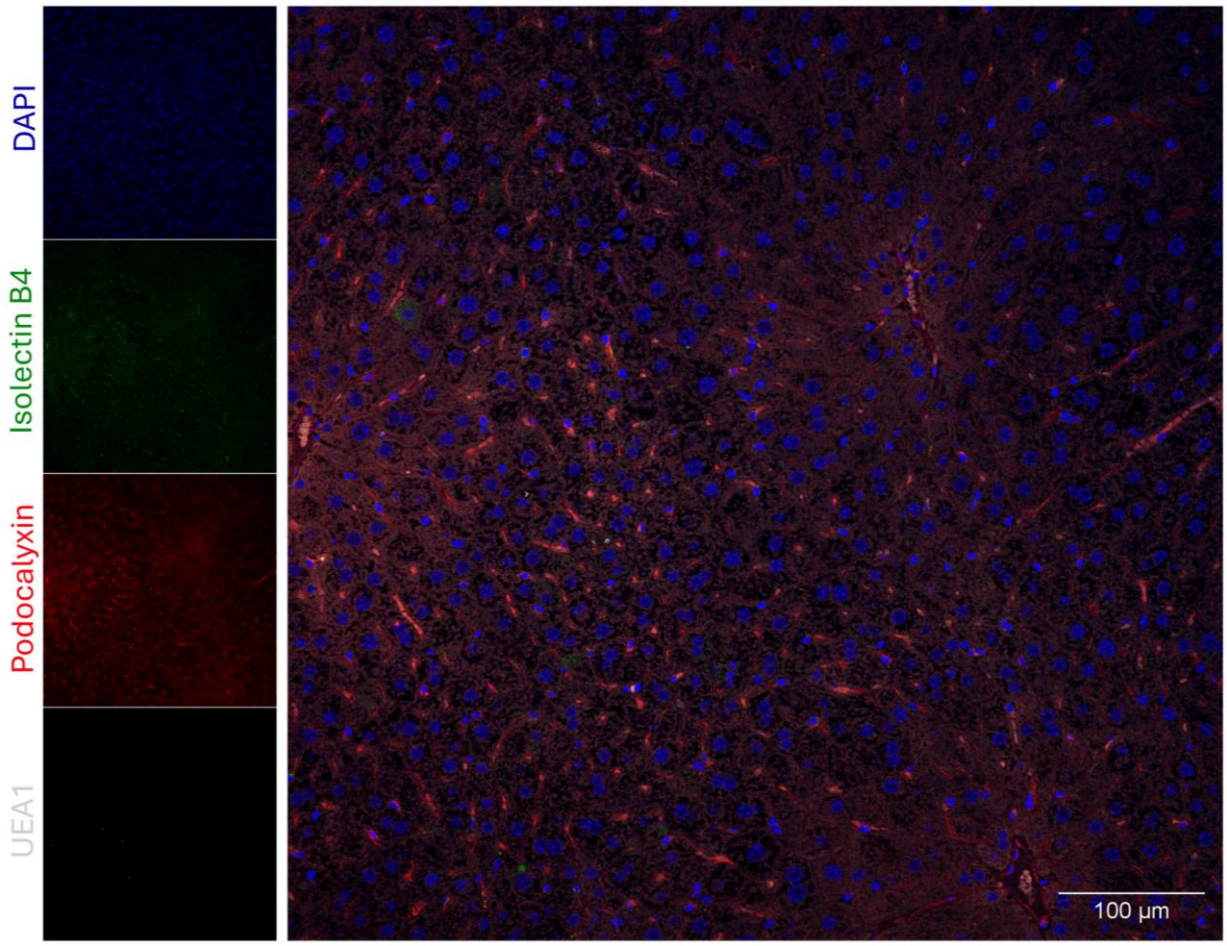

FIGURE 20. Liver tissue stained with DAPI (blue), isolectin B4 (green), podocalyxin (red), and lectin UEA1 (white/grey). Of the three known blood vessel markers, only podocalyxin stained liver tissue well. Scale bar = 100 µm.

Based on these results, we chose podocalyxin as the best vasculature marker for both pancreas and liver.

7.3.2 Changes in intra-islet capillaries associated with obesity and exercise

The analysis and results concerning the immunofluorescence staining of the liver vasculature are outside the scope of this master's thesis and will not therefore be discussed.

After the 18-week intervention, including a potential nutrition and exercise regimen, no significant differences in islet capillary density were observed between the groups (Table 5, Figure 21B). Similarly, no significant differences were found in the islet capillaries-to-nuclei ratio,

suggesting that the size of the β-cells did not change due to obesity or exercise (Figure 21C). Additionally, no significant differences were detected in islet capillary area, a variable that would indicate capillary enlargement, or in Feret's diameter, an indicator of changes in capillary size (Figure 21D–E).

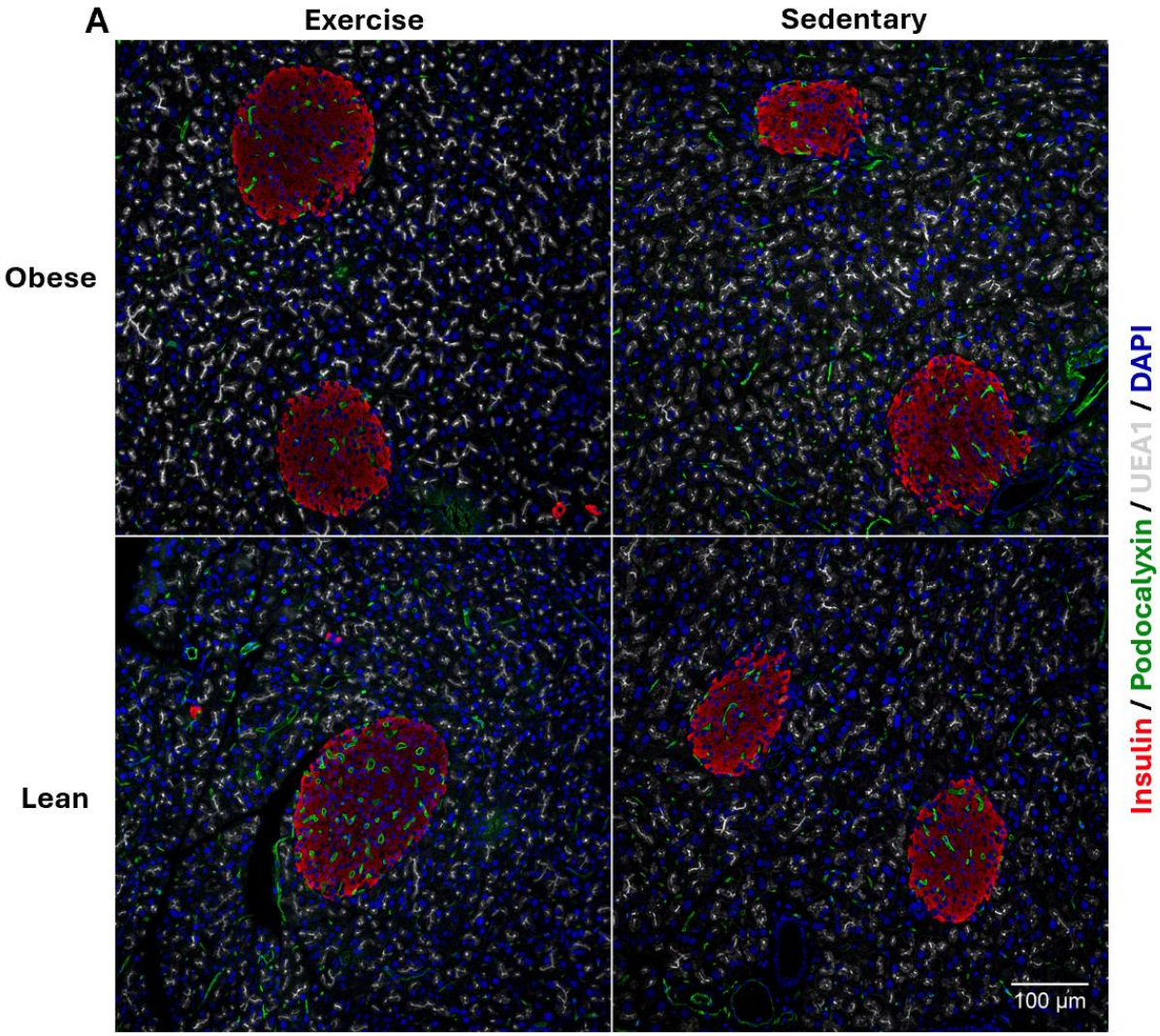

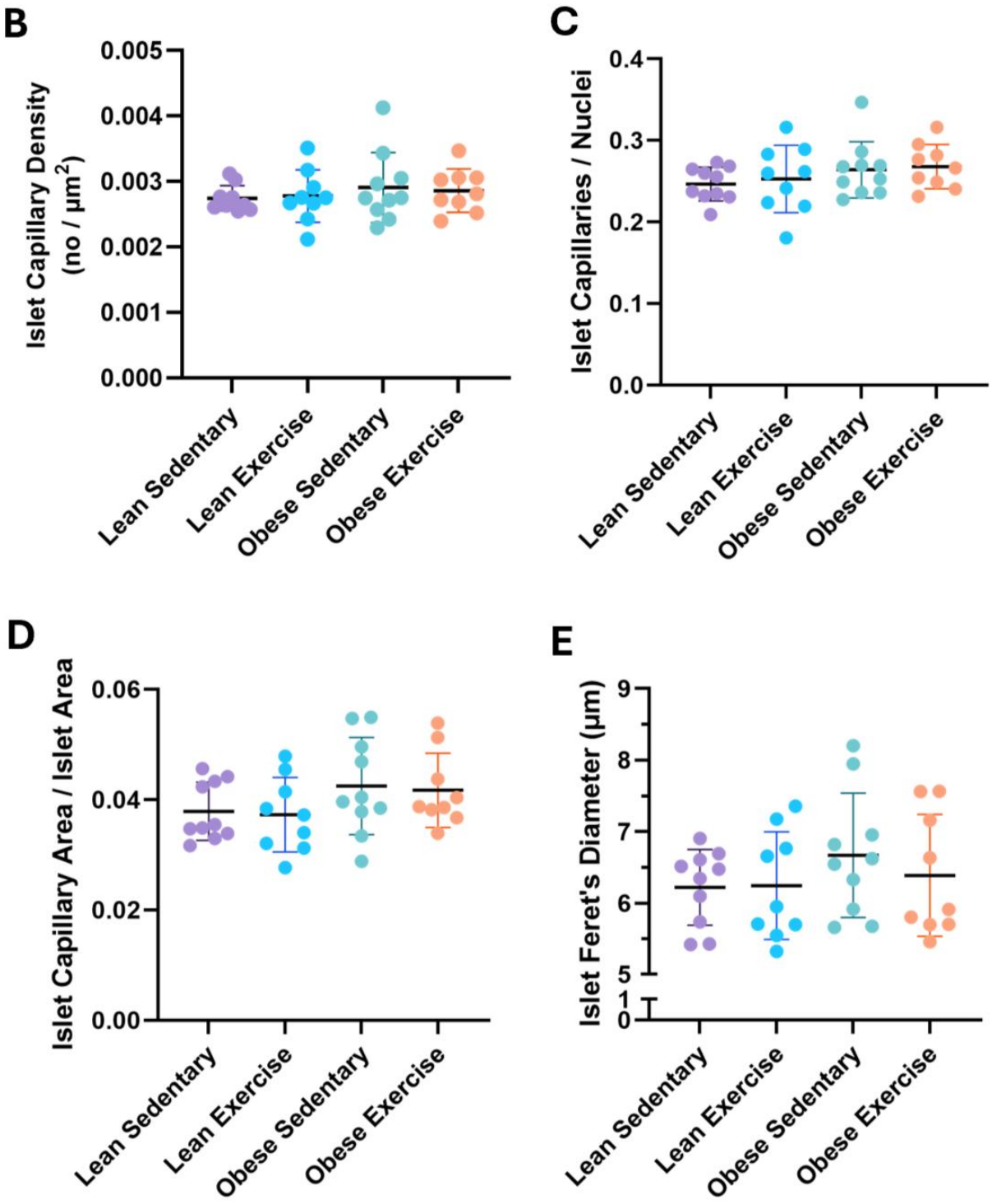

FIGURE 21. Obesity and exercise related changes in the islet capillary density, capillary / nuclei, capillary area and Feret's diameter in four mouse groups. A: Representative images of islets visualized with insulin and vasculature visualized with podocalyxin in obese exercise, obese sedentary, lean exercise and lean sedentary groups. Scale bar = 100 µm. B: islet capillary density (no / µm^2). C: capillaries-to-nuclei ratio in islet. D: Islet capillary area / islet area. E: Feret's diameter of islet capillaries (µm).

TABLE 5. P-values of islet capillary density, area, and size metrics across study groups. Statistical significance is set at P<0.05. LS = lean sedentary, LE = lean exercise, OS = obese sedentary, OE = obese exercise.

Variable	LS vs LE	LS vs OS	LS vs OE	LE vs OS	LE vs OE	OS vs OE
Capillary density	0.8534	0.3530	0.5180	0.4702	0.6519	0.7938
Capillaries / Nuclei	0.6722	0.2280	0.1521	0.4476	0.3187	0.7889
Capillary area	0.8438	0.1544	0.2463	0.1153	0.1880	0.8135
Feret's Diameter	0.9524	0.1992	0.6377	0.2330	0.6884	0.4296

Significance levels are indicated by *<0.05.

Although there were no statistically significant differences between the groups in either of the parameters, the capillary areas in the obese groups were, on average, slightly higher compared to the lean groups (Figure 21D). Furthermore, the Feret's diameter in the obese sedentary group showed greater variability, resulting in a marginally higher mean compared to the other groups (Figure 21E). All in all, there were no significant changes in any of the variables measured from the islet capillaries.

7.3.3 Changes in exocrine capillaries associated with obesity and exercise

One mouse was removed from the lean sedentary group due to significantly higher values throughout the exocrine variables, which could have affected the analysis. In contrast to the islet capillary density, where no significant differences were observed, the capillary densities of exocrine tissue in different mouse groups showed significant differences (Figure 22A, Table 6). These differences were as follows: 1) the obese sedentary group had significantly higher capillary density than both the lean exercise ($p = 0.0148$) and lean sedentary groups ($p = 0.0041$), and 2) the obese exercise group showed a significantly higher capillary density than the lean sedentary group ($p = 0.0241$). Moreover, exercise did not have a significant effect on capillary density in either lean or obese mice.

A similar trend was observed in the exocrine capillaries / nuclei variable, where the obese groups had the highest number of capillaries per nuclei (Figure 22B). The differences were significant between the obese exercise and lean exercise groups ($p = 0.0122$), obese exercise

and lean sedentary groups ($p < 0.0001$), and obese sedentary and lean sedentary groups ($p = 0.0007$). Although the difference between the lean sedentary and lean exercise groups was not statistically significant ($p = 0.0731$), the lean sedentary group had a clearly lower mean.

Regarding capillary area, an indicator of capillary enlargement, neither exercise nor obesity showed a significant effect on exocrine vasculature (Figure 22C). However, the obese groups had greater variation in their results compared to the lean groups. Additionally, the lean exercise group had slightly higher values compared to the lean sedentary group, although this difference was not statistically significant. The same trend was observed in Feret's diameter, where the obese groups had larger deviations compared to the lean groups, and the lean exercise group showed higher values than the lean sedentary group (Figure 22D). Unlike the capillary area variable, the Feret's diameter of the obese groups was smaller than that of the lean groups, suggesting the possibility of smaller capillaries in the obese groups, although these trends were not statistically confirmed.

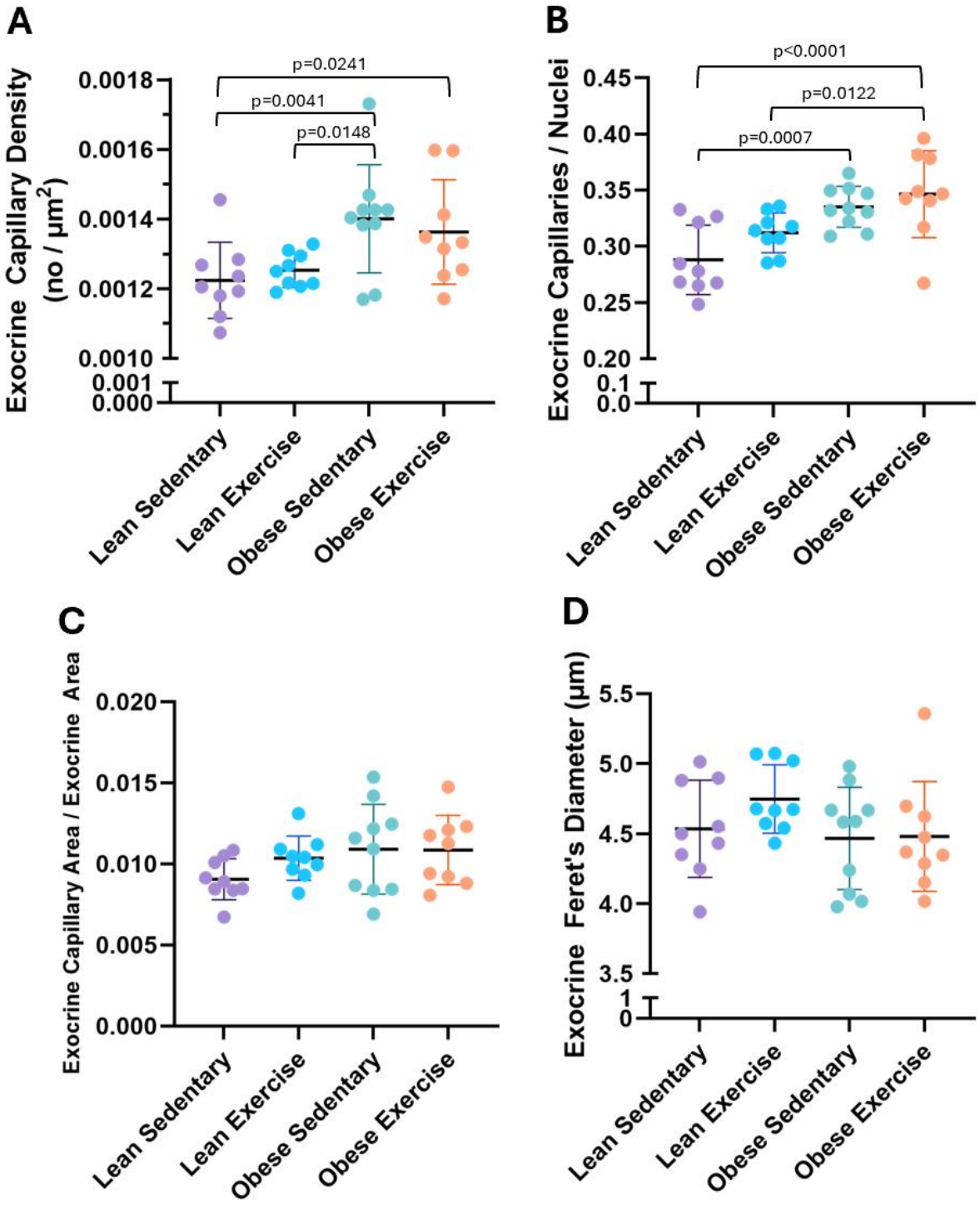

FIGURE 22. Obesity and exercise related changes in the pancreas' exocrine capillary density, capillary / nuclei, capillary area and Feret's diameter in four mouse groups. A: exocrine capillary density (no / µm^2). B: capillaries-to-nuclei ratio in exocrine tissue. C: exocrine capillary area / exocrine area. D: Feret's diameter of exocrine capillaries (µm).

TABLE 6. P-values of exocrine capillary density, area, and size metrics across study groups. Statistical significance is set at P<0.05. LS = lean sedentary, LE = lean exercise, OS = obese sedentary, OE = obese exercise.

Variable	LS vs LE	LS vs OS	LS vs OE	LE vs OS	LE vs OE	OS vs OE
Capillary density	0.6235	0.0041*	0.0241*	0.0148*	0.0705	0.5169
Capillary area	0.1784	0.0532	0.0666	0.5564	0.6052	0.9535
Capillaries / Nuclei	0.0731	0.0007**	<0.0001**	0.0769	0.0122*	0.3776
Feret's Diameter	0.1968	0.6691	0.7379	0.0838	0.1074	0.9328

Significance levels are indicated by * <0.05, and ** < 0.001.

7.3.4 Capillary density and morphology in pancreatic islet versus exocrine tissue

When comparing the capillary densities between islets and exocrine tissue of the pancreas, significant differences were observed across all groups ($p < 0.0001$) (Figure 23A). In each group, pancreatic islets had significantly higher capillary densities compared to the exocrine tissue. However, when examining the capillaries-to-nuclei ratio, exocrine tissue had consistently higher values across all mouse groups ($p < 0.0001$ to $p = 0.0029$) (Figure 23B).

Significant differences were also found in capillary area, as pancreatic islets were shown to have larger capillary area relative to tissue area compared to exocrine tissue across all groups ($p < 0.0001$). Additionally, significant differences in Feret's diameter were observed between islet and exocrine tissues across all groups ($p < 0.0001$ to $p = 0.0029$) as the pancreatic islets had consistently larger capillary Feret's diameters compared to exocrine tissues.

In conclusion, pancreatic islets exhibited higher overall capillary density, capillary area relative to tissue area, and capillary Feret's diameter compared to exocrine tissues. However, in exocrine tissue, the ratio of capillaries to nuclei was shown to be significantly higher.

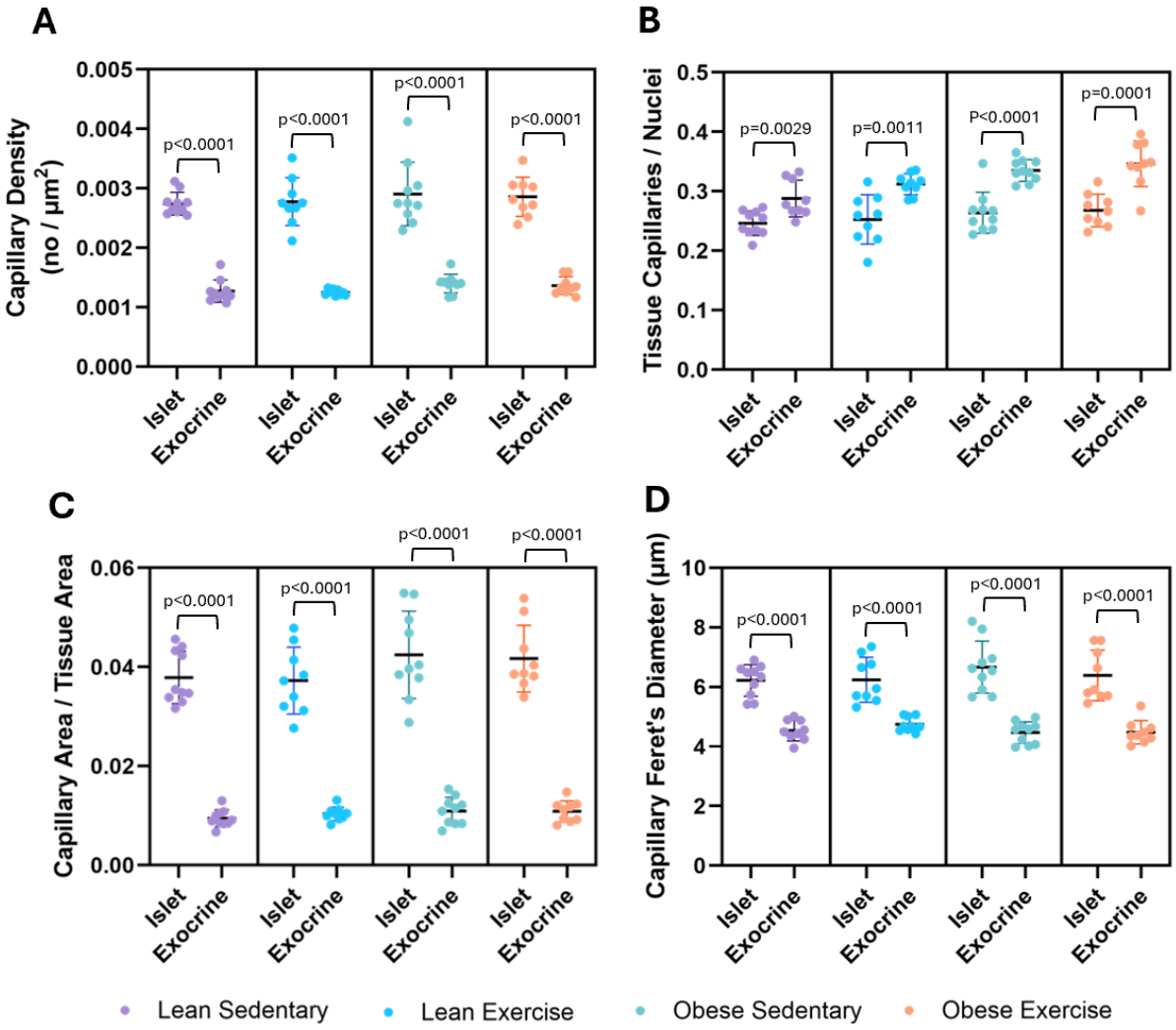

FIGURE 23. Comparison of different vascular parameters between the pancreatic islet and exocrine tissues across four mouse groups: obese exercise, obese sedentary, lean exercise, and lean sedentary. A: capillary density (no / µm^2). B: capillaries-to-nuclei ratio in chosen tissue. C: capillary area / tissue area. D: Feret's diameter of capillaries (µm).

8 DISCUSSION

In this study, pancreas tissue from obese and normal weight mice were used to study the changes in capillaries with or without exercise. The study aimed to determine whether exercise has benefits on vasculature in the context of obesity, IR and T2D.

8.1 Exercise has a positive effect on physical fitness, body weight, body composition, and glucose tolerance

The results related to the overall success of the intervention showed that the exercise has many positive effects on both physical fitness, body weight, body composition, and glucose tolerance. First, the running results of both obese and lean exercise groups were significantly improved during the intervention. Second, after introducing the running wheels, exercise prevented any additional weight gain in both obese and lean groups, whereas sedentary mice continued to add weight with age. Third, although the body weight was significantly higher throughout the experiment in both obese groups, exercising group had similar GTT results to the lean groups, highlighting the positive effect of exercise on metabolic health in obesity and prevention of T2D. These results are in line with human T2D studies that have shown that exercise can improve both insulin sensitivity, blood glucose levels, and β-cell function (Amanat et al. 2020; Heiskanen et al. 2018).

8.2 Haematoxylin-eosin staining reveals no significant pancreatic changes but highlights changes in liver tissue

No distinct differences were observed in the pancreatic sections between the mouse groups. In studies using HFD, typical histopathological changes in the pancreatic islets include hypertrophied islets and irregular islet borders (Chen et al. 2017). In the exocrine pancreas, fat deposits resembling those found in the liver can also be detected (Rugivarodom et al. 2022).

In contrast to pancreas, notable changes were observed in the liver sections, where the obese sedentary group had visibly more round-shaped, non-stained (white) areas. These round-shaped

areas are indicative of lipid accumulation (steatosis) within the liver (Ramirez-Pedraza & Fernández 2019; Tsai et al. 2020). Therefore, H&E staining demonstrated the highest lipid accumulation in the obese sedentary group. According to literature reviews by Lian et al. (2020) and Lim, Taskinen & Borén (2018), the primary driver behind hepatic fat accumulation is excessive energy intake. This aligns with our results, as the most pronounced lipid accumulation was observed in the obese group that consumed energy-rich food.

Compared to the sedentary group, exercise appeared to attenuate lipid accumulation in obese mice. This finding is consistent with previous studies using aerobic exercise protocols. For instance, in a study by Zou et al. (2021) using zebrafish, Oil Red O staining showed that sedentary HFD zebrafish had more lipid droplets in their liver compared to the exercising HFD group. Similarly, in a study by Rodrigues et al. (2022) on C57BL/6 mice, exercise reduced hepatic steatosis in T2D mice by 4.9 %. Additionally, in studies on Wistar rats (Gomes et al. 2013) and Sprague Dawley rats focusing on T2D (Carvalho et al. 2023), sedentary rats showed an apparent increase in liver fat accumulation, whereas exercise attenuated this effect—though diet had a greater impact on fat deposition than exercise. All in all, the H&E staining provides evidence of the positive effect of exercise on reducing fat accumulation, but further investigation with additional methods, such as Oil Red O dye to stain the intracellular lipids (Du et al. 2023) and quantification of the fat content within the liver tissue sections, is recommended.

8.3 Isolectin B4 and UAE1 are not suitable markers for pancreas and liver vasculature

Both isolectin B4, isolated from the Griffonia simplicifolia plant, and lectin UEA1 are carbohydrate-binding proteins that can attach to specific glycoconjugates present on cell surfaces (Cavada et al. 2022). As such, these lectins have been used in immunohistochemistry to stain blood vessels in tissues such as muscle fibers, heart, and retina in both humans and rodent models (Hutz, Degens & Korhonen 2024; Iwasaki et al. 2011; Shao et al. 2020). However, our staining results showed that neither of these markers was suitable for labelling vasculature in the pancreas or liver in our mouse model. In the pancreas, both markers stained structures outside the islet of Langerhans, which did not colocalize with vascular marker podocalyxin, whereas in the liver, neither marker stained any structures.

Upon reviewing the literature, it was confirmed that in the mouse pancreas, UEA1 does not stain the blood vessels in the mouse pancreas but instead it has an affinity for acinar cells (Xiao et al. 2016), a cell type responsible for synthesizing, storing, and secreting digestive enzymes into the small intestine (Leung & Ip 2006). Additionally, GSL1, a lectin isolated from Griffonia simplicifolia and therefore similar to isolectin B4, has been shown to have strong affinity for acinar cells and only weak affinity for endothelial labelling (Xiao et al. 2016). Furthermore, although many lectins bind to the microvascular wall of the mouse liver, fucose-binding lectins, such as our UEA1, and N-acetyl-D-galactosamine-binding lectins, such as our isolectin B4, were found not to attach to the endothelial surface of the mouse liver microvasculature (Barberá-Guillem et al. 1991). These findings further demonstrate the versatile nature of blood vessels in different parts of the body.

In conclusion, our findings align with the previous studies showing that neither isolectin B4 nor lectin UEA1 are suitable blood vessel markers in the pancreas or liver, thereby reinforcing earlier findings. Although these markers are not suitable for blood vessels in the pancreas or liver, it should be noted that they can still be useful in other tissues or as markers for other structures, such as UEA1 for acinar cells.

8.4 Obesity and exercise show no significant effect on pancreatic islet capillaries

Several rodent studies have reported conflicting results regarding ICD, with findings showing no changes (Castillo et al. 2022; Mizuno et al. 1999), a decrease (Castillo et al. 2022; Dai et al. 2013; Li et al. 2006; Mizuno et al. 1999; Nakamura et al. 1995), or an increase in ICD (Castillo et al. 2022; Okajima et al. 2022) in response to obesity and weight gain. In our study, we observed no significant differences in ICD among any of the mouse groups. This lack of difference may be due to several factors. Firstly, previous research outcomes seem to be influenced by the specific rodent model used, the age of the animals, and the severity of T2D, as rodents with advanced age or more severe T2D have more often shown a decrease in ICD (Castillo et al. 2022; Dai et al. 2013; Li et a. 2006; Mizuno et al. 1999). Thus, our results might have differed had the intervention been longer, potentially leading to more severe IR and T2D, and consequently more pronounced vascular changes. Moreover, recent studies focusing on amyloid deposits in both rodents and humans have shown a selective decrease in ICD in areas close to the amyloid deposits (Castillo et al. 2022; Ling et al. 2020). Therefore, future studies investigating

changes in ICD should take into account the amyloid deposits before drawing any further conclusions about the effects of obesity and T2D on ICD.

Previous studies have generally shown that islet capillaries dilate in response to IR and T2D in both rodents and humans (Agudo et al. 2012; Dai et al. 2013; Hogan et al. 2017; Li et al. 2006; Okajima et al. 2022; Takahashi et al. 2021). However, in our findings, capillary area and Feret's diameter – both indicators of capillary enlargement – were not significantly different among the groups. Despite this, there was a trend toward larger capillary areas in both obese groups and higher Feret's diameter values in the obese sedentary group compared to the other three groups. This trend suggests that subtle vascular changes may have occurred in response to obesity and IR, and that exercise might mitigate these changes, particularly in Feret's diameter. It is possible that a longer intervention duration could have resulted in more pronounced changes, potentially leading to more severe IR and T2D, and clearer effects on capillary expansion. Future research with extended intervention periods could further illustrate the role of exercise in mitigating capillary enlargement and reveal more significant differences.

8.5 Obesity increases capillary density in pancreatic exocrine tissue

To our surprise, significant differences were observed between mouse groups in capillary density and the capillary-to-nuclei ratio within the exocrine tissue of the pancreas due to obesity. The obese groups exhibited higher means than the lean groups, suggesting that increased energy intake and overweight might increase the number of capillaries in the exocrine tissue. This finding is in contrast with a previous study involving ob/ob mice (Dai et al. 2013), where researchers concluded that the vasculature of exocrine tissue remained unchanged in insulin-resistant ob/ob mice. Their conclusion was further supported by a test using lectin-FITC labeling, which co-localized with endothelial cell markers such as CD31 and caveolin-1, confirming that the blood vessels were quiescent and not forming new sprouts.

To validate our contrasting results, a similar approach to that of Dai et al. (2013) could be employed to determine whether the blood vessels in our study are indeed not in a quiescent state. However, it is important to note that during the literature review, no other studies were found that specifically examined the exocrine tissue during obesity or T2D. While some studies focused on the density of peri-islet capillaries – vessels adjacent to both endocrine and exocrine

tissue – these capillaries are not equivalent to those in the exocrine tissue (Brissova et al. 2015; Hayden et al. 2008). Thus, the effects of obesity, IR or T2D on exocrine vasculature needs further studies, but the findings of this thesis suggest that obesity has stronger effect on the exocrine than on the endocrine vasculature.

Although no significant results were found in the capillary area or Feret's diameter, some intriguing trends emerged between the obese and lean groups. In the obese groups, the mean Feret's diameter was smaller compared to the lean groups, suggesting the possibility of smaller capillaries in the obese groups. When combined with the higher capillary density observed in the obese groups, this finding could indicate that intussusceptive angiogenesis—also known as splitting angiogenesis—may have occurred. In this type of angiogenesis, endothelial cells extend into the lumen, thus splitting the vessel into two separate blood vessels (Dudley & Griffioen 2023). As a result, the number of capillaries increases, but the diameter of individual vessels decreases. This process would explain why no changes were observed in capillary area, aligning with our results. To further investigate this hypothesis, RNA analysis could be conducted to examine the molecular mechanisms underlying these vascular changes.

Regarding the effects of exercise, it did not appear to influence any of the measured parameters. This could be due to at least one reason. In general, blood flow to each tissue is regulated according to the tissue's needs. When a tissue is active, more oxygen-rich blood is delivered to it (Hall & Guyton 2011, 158). During exercise, skeletal muscles are highly active, which increases the proportion of cardiac output directed toward them from approximately 20 % to as much as 85 % (Olver et al. 2015). In contrast, blood flow to internal organs is substantially reduced during exercise (Perko et al. 1998). In active skeletal muscles, exercise-induced angiogenesis is well-established, leading to an increase in capillary density over time (Olfert et al. 2016). According to reviews by Green et al. (2017) and Olfert et al. (2016), one of the mechanisms that initiate exercise-induced angiogenesis is the significant increase in blood flow through skeletal muscles. This increase generates mechanical stimulus, such as heightened shear stress, stretch, and pressure on the vascular walls of the exercising muscles, which then initiates the vascular adaptations by mediating the release of angiogenic growth factors. It could therefore be hypothesized that in internal organs, such as the pancreas, no such changes occur during exercise, as blood flow is substantially reduced, and consequently, the capillary walls of the pancreas do not experience similar stress, stretch, or pressure that is present in the exercising muscles during physical activity. However, although no significant changes were observed due

to exercise, it should be noted that, as mentioned earlier, a longer duration of the intervention could have resulted in more pronounced changes.

8.6 Distinct vascular differences between pancreatic islet and exocrine tissue

Our results show that pancreatic islets have significantly higher capillary densities compared to exocrine tissue, regardless of the mouse group. Specifically, the islets were found to be approximately twice as densely vascularized as the corresponding exocrine tissue. This suggests that islet tissues are more densely vascularized than exocrine tissues across all conditions, whether obese or lean, exercised or sedentary. These findings align with a study by Brissova et al. (2006), which also reported that the density of intra-islet capillaries was twice as great compared to exocrine tissue. However, when examining the number of capillaries-to-nuclei ratio, our results showed a different pattern, indicating that the exocrine tissue had a higher ratio of capillaries to nuclei. This is likely due to larger cell size in the exocrine tissue. This interpretation is supported by figures showing the DAPI staining of the pancreas tissues (Figures 18 and 19), which show that the nuclei in the islets are visibly smaller and more tightly packed, whereas in the exocrine tissue, the nuclei are larger and more spaced apart.

Regarding Feret's diameter — a measure that provides an indication of capillary width — our results show that the capillaries within the islets had consistently higher values compared to those in the exocrine tissue. This suggests that islet capillaries are wider than those in exocrine tissue under all conditions. These findings are consistent with previous studies (Vetterlein, Pethö & Schmidt 1987; Henderson & Moss 1985; Bonner-Weir & Orci 1982), which reported similar differences. In our study, the average Feret's diameter of all mice was 6,38 ± 0.8 μm in the islets and 4,55 ± 0.3 μm in the exocrine tissue. This is comparable to the studies by Henderson and Moss (1985) and Vetterlein, Pethö & Schmidt (1987), where in the former, the mean capillary diameter in endocrine capillaries was 5.27 ± 0.22 μm, and in exocrine capillaries it was 4.35 ± 0.3 μm, and in the latter, the mean capillary diameter was 6.7 ± 0.2 μm, and 5.7 ± 0.2 μm, respectively. The difference in capillary area also makes sense, as the exocrine tissue has both fewer and smaller capillaries, naturally occupying less space.

In summary, pancreatic islets consistently showed higher vascularization compared to exocrine tissue, indicating that islets are both more vascularized and have larger capillaries. Also, these

results suggest that the differences in vascularization between islet and exocrine tissues are consistent and not significantly affected by obesity or exercise.

8.7 Strengths and limitations of this study

8.7.1 Strengths

The study was conducted with sufficiently large mouse groups to yield statistically significant results. Additionally, unlike humans, where pancreas and liver samples are often obtained post-mortem under less standardized conditions, in mice, the conditions and mouse type can be controlled, providing a more uniform study environment.

The intervention was successful, as demonstrated by the findings that the energy-rich diet induced obesity and IR, while the exercise protocol produced positive effects on physical fitness, body weight, body composition, and glucose tolerance. Therefore, the results from both the pancreas and liver can be confidently interpreted, knowing that the intervention itself was successful. Also, regarding the pancreas, the image analysis was performed using a code developed specifically for these samples, which minimized variation between the analysis of different tissue sections.

8.7.2 Limitations

Firstly, although the study was carefully conducted, it did not specify the exact region (duodenal, splenic, or gastric lobe) of the pancreas from which the pancreas sections were taken. While some studies have employed a regional approach (Hull et al. 2005; Wang et al. 2001), this is not always the case (Dai et al. 2013; Okajima et al. 2022), suggesting that our methodology is still valid. However, this lack of regional specificity could introduce variability in the results.

Additionally, the study only assessed outcomes at the end of the intervention, which limits our ability to track changes in β-cell size over time. It is well-documented that β-cell mass initially increases significantly to compensate and prevent the development of T2D but then decreases

in size as the disease progresses (Chen et al. 2017). These changes could potentially influence capillary density and other vascular measurements.

Recent studies have observed a relationship between amyloid deposits and capillary density in the pancreas. For instance, Ling et al. (2020) and Castillo et al. (2022) reported a selective decrease in ICD when amyloid deposits were considered, suggesting a negative impact on vascular density in vivo. However, our study did not account for amyloid deposits. According to Wang et al. (2001), rodent islet amyloid polypeptide (IAPP) is non-amyloidogenic meaning that islet amyloid does not naturally occur in in normal mice and rats. Therefore, to study amyloid deposits in rodent models, transgenic mice are typically required. Since our study used normal C57BL/6J adult male mice, this could explain the absence of capillary rarefaction in our results. Investigating the presence of amyloid deposits in an appropriate model could provide further insights into our findings.

In addition to these limitations, the study utilized only two staining procedures: H&E and immunofluorescence. To further validate our results, additional methods should be employed. First, we did not measure pancreatic blood flow, which has been shown to be affected in obese-hyperglycemic ob/ob mice (Carlsson, Andersson & Jansson 1996; Dai et al. 2013; Okajima et al. 2022). Therefore, we cannot make any conclusions about the functionality of the blood vessels observed in our study. This is particularly relevant in the exocrine tissue, where we noted a potential increase in capillary density due to obesity. Additionally, due to the thin tissue sections used, it was not possible to assess the 3D structure of the capillaries, which some studies have described as meandering due to obesity (Okajima et al. 2022).

8.8 Summary

This study aimed to determine whether exercise affects internal organs pancreas and liver in the context of obesity, IR and T2D, a topic that is rarely explored despite exercise being commonly prescribed as a type of treatment for these conditions. The exercise intervention effectively prevented additional weight gain in both obese and lean mice and improved glucose tolerance in the obese exercising mice, highlighting the benefits of physical activity in preventing obesity and T2D. Additionally, the H&E-stained liver tissue showed clear differences between

lean and obese groups, with exercise reducing lipid accumulation in the liver, aligning with previous findings on the benefits of exercise in managing hepatic steatosis.

In islets, no significant differences were found regarding capillary density or capillary enlargement. However, there was a trend toward possible capillary enlargement in obese groups, suggesting that subtle vascular changes might be occurring and could potentially become significant over time. Also, in Feret's diameter, obese exercise mice had values closer to that of lean groups, therefore suggesting that exercise could potentially mitigate these changes in longer intervention.

In exocrine tissue, obesity significantly increased capillary density and the capillary-to-nuclei ratio, suggesting that increased energy intake and overweight may lead to more capillaries in this tissue area. The slightly smaller Feret's diameter in obese groups, despite higher capillary density, suggests that intussusceptive angiogenesis might be occurring, resulting in smaller individual capillaries. Further studies, including RNA analysis, are needed to explore the molecular mechanisms behind these vascular changes. In exocrine tissue, exercise did not seem to impact the measured parameters.

In future studies, the influence of amyloid deposits should be considered when investigating the vascular changes in islets. Additionally, a longer intervention period could potentially reveal more pronounced effects and better illustrate the role of exercise in mitigating the changes in vasculature.

REFERENCES

Agudo, J., Ayuso, E., Jimenez, V., Casellas, A., Mallol, C., Salavert, A., Tafuro, S., Obach, M., Ruzo, A., Moya, M., Pujol, A. & Bosch, F. (2012). Vascular endothelial growth factor-mediated islet hypervascularization and inflammation contribute to progressive reduction of β-cell mass. Diabetes 61 (11), 2851–2861. doi:10.2337/db12-0134.

Almaça, J., Weitz, J., Rodriguez-Diaz, R., Pereira, E. & Caicedo, A. (2018). The Pericyte of the Pancreatic Islet Regulates Capillary Diameter and Local Blood Flow. Cell metabolism 27 (3), 630–644.e4. doi:10.1016/j.cmet.2018.02.016.

Amanat, S., Ghahri, S., Dianatinasab, A., Fararouei, M. & Dianatinasab, M. (2020). Exercise and Type 2 Diabetes. Advances in experimental medicine and biology 1228, 91–105. doi:10.1007/978-981-15-1792-1_6.

Barberá-Guillem, E., Rocha, M., Alvarez, A. & Vidal-Vanaclocha, F. (1991). Differences in the lectin-binding patterns of the periportal and perivenous endothelial domains in the liver sinusoids. Hepatology (Baltimore, Md.) 14 (1), 131–139. doi:10.1002/hep.1840140122.

Bonner-Weir, S. & Orci, L. (1982). New perspectives on the microvasculature of the islets of Langerhans in the rat. Diabetes 31 (10), 883–889. doi:10.2337/diab.31.10.883.

Bosco, D., Armanet, M., Morel, P., Niclauss, N., Sgroi, A., Muller, Y. D., Giovannoni, L., Parnaud, G. & Berney, T. (2010). Unique arrangement of alpha- and beta-cells in human islets of Langerhans. Diabetes 59 (5), 1202–1210. doi:10.2337/db09-1177.

Brissova, M., Fowler, M. J., Nicholson, W. E., Chu, A., Hirshberg, B., Harlan, D. M. & Powers, A. C. (2005). Assessment of human pancreatic islet architecture and composition by laser scanning confocal microscopy. The journal of histochemistry and cytochemistry : official journal of the Histochemistry Society 53 (9), 1087–1097. doi:10.1369/jhc.5C6684.2005.

Brissova, M., Shostak, A., Fligner, C. L., Revetta, F. L., Washington, M. K., Powers, A. C., & Hull, R. L. (2015). Human Islets Have Fewer Blood Vessels than Mouse Islets and the Density of Islet Vascular Structures Is Increased in Type 2 Diabetes. The journal of histochemistry and cytochemistry : official journal of the Histochemistry Society 63 (8), 637–645. doi:10.1369/0022155415573324.

Brissova, M., Shostak, A., Shiota, M., Wiebe, P. O., Poffenberger, G., Kantz, J., Chen, Z., Carr, C., Jerome, W. G., Chen, J., Baldwin, H. S., Nicholson, W., Bader, D. M., Jetton, T., Gannon, M. & Powers, A. C. (2006). Pancreatic islet production of vascular

endothelial growth factor--a is essential for islet vascularization, revascularization, and function. Diabetes 55 (11), 2974–2985. doi:10.2337/db06-0690.

Burke, S. J., Batdorf, H. M., Burk, D. H., Noland, R. C., Eder, A. E., Boulos, M. S., Karlstad, M. D. & Collier, J. J. (2017). db/db Mice Exhibit Features of Human Type 2 Diabetes That Are Not Present in Weight-Matched C57BL/6J Mice Fed a Western Diet. Journal of diabetes research 8503754. doi:10.1155/2017/8503754.

Butler, A. E., Jang, J., Gurlo, T., Carty, M. D., Soeller, W. C. & Butler, P. C. (2004). Diabetes due to a progressive defect in beta-cell mass in rats transgenic for human islet amyloid polypeptide (HIP Rat): a new model for type 2 diabetes. Diabetes 53 (6), 1509–1516. doi:10.2337/diabetes.53.6.1509.

Butler, A. E., Janson, J., Bonner-Weir, S., Ritzel, R., Rizza, R. A. & Butler, P. C. (2003). Beta-cell deficit and increased beta-cell apoptosis in humans with type 2 diabetes. Diabetes 52 (1), 102–110. doi:10.2337/diabetes.52.1.102.

Cabrera, O., Berman, D. M., Kenyon, N. S., Ricordi, C., Berggren, P. O. & Caicedo, A. (2006). The unique cytoarchitecture of human pancreatic islets has implications for islet cell function. Proceedings of the National Academy of Sciences of the United States of America 103 (7), 2334–2339. doi:10.1073/pnas.0510790103.

Carlsson, P. O., Andersson, A. & Jansson, L. (1996). Pancreatic islet blood flow in normal and obese-hyperglycemic (ob/ob) mice. The American journal of physiology 271 (6 Pt 1), E990–E995. doi:10.1152/ajpendo.1996.271.6.E990.

Carvalho, V. H. C., Wang, Q., Xu, X., Liu, L., Jiang, W., Wang, X., Wang, J., Li, W., Chen, J., Li, T., Chen, Y., Zhu, W., Sun, Z. & Qiu, S. (2023). Long-term exercise preserves pancreatic islet structure and β-cell mass through attenuation of islet inflammation and fibrosis. FASEB journal : official publication of the Federation of American Societies for Experimental Biology 37 (3), e22822. doi:10.1096/fj.202201879R.

Castillo, J. J., Aplin, A. C., Hackney, D. J., Hogan, M. F., Esser, N., Templin, A. T., Akter, R., Kahn, S. E., Raleigh, D. P., Zraika, S. & Hull, R. L. (2022). Islet amyloid polypeptide aggregation exerts cytotoxic and proinflammatory effects on the islet vasculature in mice. Diabetologia 65 (10), 1687–1700. doi:10.1007/s00125-022-05756-9.

Cavada, B. S., Pinto-Junior, V. R., Osterne, V. J. S., Oliveira, M. V., Silva, I. B., Laranjeira, E. P. P., Pires, A. F., Domingos, J. L. C., Ferreira, W. P., Sousa, J. S., Assreuy, A. M. S. & Nascimento, K. S. (2022). In depth analysis on the carbohydrate-binding properties

of a vasorelaxant lectin from Dioclea lasiophylla Mart Ex. Benth seeds. Journal of biomolecular structure & dynamics 40 (15), 6817–6830. doi:10.1080/07391102.2021.1890224.

Chen, C., Cohrs, C. M., Stertmann, J., Bozsak, R. & Speier, S. (2017). Human beta cell mass and function in diabetes: Recent advances in knowledge and technologies to understand disease pathogenesis. Molecular metabolism 6 (9), 943–957. doi:10.1016/j.molmet.2017.06.019.

Clark, A., Wells, C. A., Buley, I. D., Cruickshank, J. K., Vanhegan, R. I., Matthews, D. R., Cooper, G. J., Holman, R. R. & Turner, R. C. (1988). Islet amyloid, increased A-cells, reduced B-cells and exocrine fibrosis: quantitative changes in the pancreas in type 2 diabetes. Diabetes research (Edinburgh, Scotland) 9 (4), 151–159.

Colberg, S. R., Sigal, R. J., Fernhall, B., Regensteiner, J. G., Blissmer, B. J., Rubin, R. R., Chasan-Taber, L., Albright, A. L., Braun, B., American College of Sports Medicine, & American Diabetes Association (2010). Exercise and type 2 diabetes: the American College of Sports Medicine and the American Diabetes Association: joint position statement. Diabetes care 33(12), e147–e167. doi:10.2337/dc10-9990.

Cristi-Montero, C., Chillón, P., Labayen, I., Casajus, J. A., Gonzalez-Gross, M., Vanhelst, J., Manios, Y., Moreno, L. A., Ortega, F. B., Ruiz, J. R. & HELENA study group (2019). Cardiometabolic risk through an integrative classification combining physical activity and sedentary behavior in European adolescents: HELENA study. Journal of sport and health science 8 (1), 55–62. doi:10.1016/j.jshs.2018.03.004.

Da Silva, X. G. (2018). The Cells of the Islets of Langerhans. Journal of clinical medicine 7 (3), 54. doi:10.3390/jcm7030054.

Dai, C., Brissova, M., Reinert, R. B., Nyman, L., Liu, E. H., Thompson, C., Shostak, A., Shiota, M., Takahashi, T. & Powers, A. C. (2013). Pancreatic islet vasculature adapts to insulin resistance through dilation and not angiogenesis. Diabetes 62 (12), 4144–4153. doi:10.2337/db12-1657.

de Waard, A. M., Hollander, M., Korevaar, J. C., Nielen, M. M. J., Carlsson, A. C., Lionis, C., Seifert, B., Thilsing, T., de Wit, N. J., Schellevis, F. G. & SPIMEU Project Group (2019). Selective prevention of cardiometabolic diseases: activities and attitudes of general practitioners across Europe. European journal of public health 29 (1), 88–93. doi:10.1093/eurpub/cky112.

Dludla, P. V., Mabhida, S. E., Ziqubu, K., Nkambule, B. B., Mazibuko-Mbeje, S. E., Hanser, S., Basson, A. K., Pheiffer, C. & Kengne, A. P. (2023). Pancreatic β-cell dysfunction in

type 2 diabetes: Implications of inflammation and oxidative stress. World journal of diabetes 14 (3), 130–146. doi:10.4239/wjd.v14.i3.130.

Dolenšek, J., Rupnik, M. S. & Stožer, A. (2015). Structural similarities and differences between the human and the mouse pancreas. Islets 7 (1), e1024405. doi:10.1080/19382014.2015.1024405.

Du, J., Zhao, L., Kang, Q., He, Y. & Bi, Y. (2023). An optimized method for Oil Red O staining with the salicylic acid ethanol solution. Adipocyte 12 (1), 2179334. doi:10.1080/21623945.2023.2179334.

Dudley, A. C. & Griffioen, A. W. (2023). The modes of angiogenesis: an updated perspective. Angiogenesis 26 (4), 477–480. doi:10.1007/s10456-023-09895-4.

Fowler, J. L., Lee, S. S., Wesner, Z. C., Olehnik, S. K., Kron, S. J. & Hara, M. (2018). Three-Dimensional Analysis of the Human Pancreas. Endocrinology 159 (3), 1393–1400. doi:10.1210/en.2017-03076.

Galicia-Garcia, U., Benito-Vicente, A., Jebari, S., Larrea-Sebal, A., Siddiqi, H., Uribe, K. B., Ostolaza, H. & Martín, C. (2020). Pathophysiology of Type 2 Diabetes Mellitus. International journal of molecular sciences 21 (17), 6275. doi:10.3390/ijms21176275.

Gomes, R. M., Tófolo, L. P., Rinaldi, W., Scomparin, D. X., Grassiolli, S., Barella, L. F., de Oliveira, J. C., Branco, R. C., Agostinho, A. R., Ribeiro, T. A., Gravena, C. & Mathias, P. C. (2013). Moderate exercise restores pancreatic beta-cell function and autonomic nervous system activity in obese rats induced by high-fat diet. Cellular physiology and biochemistry : international journal of experimental cellular physiology, biochemistry, and pharmacology 32 (2), 310–321. doi:10.1159/000354439.

Grapin-Botton, A. (2005). Ductal cells of the pancreas. The international journal of biochemistry & cell biology 37 (3), 504–510. doi:10.1016/j.biocel.2004.07.010.

Green, D. J., Hopman, M. T. E., Padilla, J., Laughlin, M. H. & Thijssen, D. H. J. (2017). Vascular Adaptation to Exercise in Humans: Role of Hemodynamic Stimuli. Physiological Reviews 97 (2), 495–528. doi:10.1152/physrev.00014.2016.

Green, D. J. & Smith, K. J. (2018). Effects of Exercise on Vascular Function, Structure, and Health in Humans. Cold Spring Harbor perspectives in medicine 8 (4), a029819. doi:10.1101/cshperspect.a029819.

Hall, J. E. & Guyton, A. C. (2011). Guyton and Hall textbook of medical physiology (12th ed.). Saunders Elsevier.

Hayden, M. R., Karuparthi, P. R., Habibi, J., Lastra, G., Patel, K., Wasekar, C., Manrique, C. M., Ozerdem, U., Stas, S. & Sowers, J. R. (2008). Ultrastructure of islet microcirculation, pericytes and the islet exocrine interface in the HIP rat model of diabetes. Experimental biology and medicine (Maywood, N.J.) 233 (9), 1109–1123. doi:10.3181/0709-RM-251.

Heiskanen, M. A., Motiani, K. K., Mari, A., Saunavaara, V., Eskelinen, J. J., Virtanen, K. A., Koivumäki, M., Löyttyniemi, E., Nuutila, P., Kalliokoski, K. K. & Hannukainen, J. C. (2018). Exercise training decreases pancreatic fat content and improves beta cell function regardless of baseline glucose tolerance: a randomised controlled trial. Diabetologia 61 (8), 1817–1828. doi:10.1007/s00125-018-4627-x.

Henderson, J. R. & Moss, M. C. (1985). A morphometric study of the endocrine and exocrine capillaries of the pancreas. Quarterly journal of experimental physiology (Cambridge, England) 70 (3), 347–356. doi:10.1113/expphysiol.1985.sp002920.

Hogan, M. F. & Hull, R. L. (2017). The islet endothelial cell: a novel contributor to beta cell secretory dysfunction in diabetes. Diabetologia 60 (6), 952–959. doi:10.1007/s00125-017-4272-9.

Hogan, M. F., Liu, A. W., Peters, M. J., Willard, J. R., Rabbani, Z., Bartholomew, E. C., Ottley, A. & Hull, R. L. (2017). Markers of Islet Endothelial Dysfunction Occur in Male B6.BKS(D)-Leprdb/J Mice and May Contribute to Reduced Insulin Release. Endocrinology 158 (2), 293–303. doi:10.1210/en.2016-1393.

Huang, H. H., Harrington, S. & Stehno-Bittel, L. (2018). The Flaws and Future of Islet Volume Measurements. Cell transplantation 27 (7), 1017–1026. doi:10.1177/0963689718779898.

Hull, R. L., Shen, Z. P., Watts, M. R., Kodama, K., Carr, D. B., Utzschneider, K. M., Zraika, S., Wang, F., & Kahn, S. E. (2005). Long-term treatment with rosiglitazone and metformin reduces the extent of, but does not prevent, islet amyloid deposition in mice expressing the gene for human islet amyloid polypeptide. Diabetes 54 (7), 2235–2244. doi:10.2337/diabetes.54.7.2235.

Hutz, B., Degens, H. & Korhonen, M. T. (2024). Oldies, but goldies-preserved morphology and stability of antigenic determinants in decades-old cryosections of human m. vastus lateralis. Journal of anatomy 244 (5), 882–886. doi:10.1111/joa.14003.

Ionescu-Tirgoviste, C., Gagniuc, P. A., Gubceac, E., Mardare, L., Popescu, I., Dima, S. & Militaru, M. (2015). A 3D map of the islet routes throughout the healthy human pancreas. Scientific reports 5, 14634. doi:10.1038/srep14634.

Iwasaki, H., Kawamoto, A., Tjwa, M., Horii, M., Hayashi, S., Oyamada, A., Matsumoto, T., Suehiro, S., Carmeliet, P. & Asahara, T. (2011). PlGF repairs myocardial ischemia through mechanisms of angiogenesis, cardioprotection and recruitment of myo-angiogenic competent marrow progenitors. PloS one 6 (9), e24872. doi:10.1371/journal.pone.0024872.

Jansson, L. & Carlsson, P. O. (2002). Graft vascular function after transplantation of pancreatic islets. Diabetologia 45 (6), 749–763. doi:10.1007/s00125-002-0827-4.

Jansson, L. & Hellerström, C. (1983). Stimulation by glucose of the blood flow to the pancreatic islets of the rat. Diabetologia 25 (1), 45–50. doi:10.1007/BF00251896.

Kanaley, J. A., Colberg, S. R., Corcoran, M. H., Malin, S. K., Rodriguez, N. R., Crespo, C. J., Kirwan, J. P. & Zierath, J. R. (2022). Exercise/Physical Activity in Individuals with Type 2 Diabetes: A Consensus Statement from the American College of Sports Medicine. Medicine and science in sports and exercise 54 (2), 353–368. doi:10.1249/MSS.0000000000002800.

Leung, P. S. & Ip, S. P. (2006). Pancreatic acinar cell: its role in acute pancreatitis. The international journal of biochemistry & cell biology 38(7), 1024–1030. doi:10.1016/j.biocel.2005.12.001.

Levetan, C. S. & Pierce, S. M. (2013). Distinctions between the islets of mice and men: implications for new therapies for type 1 and 2 diabetes. Endocrine practice : official journal of the American College of Endocrinology and the American Association of Clinical Endocrinologists 19 (2), 301–312. doi:10.4158/EP12138.RA.

Li, X., Zhang, L., Meshinchi, S., Dias-Leme, C., Raffin, D., Johnson, J. D., Treutelaar, M. K. & Burant, C. F. (2006). Islet microvasculature in islet hyperplasia and failure in a model of type 2 diabetes. Diabetes 55 (11), 2965–2973. doi:10.2337/db06-0733.

Lian, C. Y., Zhai, Z. Z., Li, Z. F. & Wang, L. (2020). High fat diet-triggered non-alcoholic fatty liver disease: A review of proposed mechanisms. Chemico-biological interactions 330, 109199. doi:10.1016/j.cbi.2020.109199.

Lim, S., Taskinen, M. R. & Borén, J. (2019). Crosstalk between nonalcoholic fatty liver disease and cardiometabolic syndrome. Obesity reviews: an official journal of the International Association for the Study of Obesity 20 (4), 599–611. doi:10.1111/obr.12820.

Ling, W., Huang, Y., Huang, Y. M., Shen, J., Wang, S. H. & Zhao, H. L. (2020). Pancreatic Angiopathy Associated With Islet Amyloid and Type 2 Diabetes Mellitus. Pancreas 49 (9), 1232–1239. doi:10.1097/MPA.0000000000001664.

Mateus Gonçalves, L., Pereira, E., Werneck de Castro, J. P., Bernal-Mizrachi, E. & Almaça, J. (2020). Islet pericytes convert into profibrotic myofibroblasts in a mouse model of islet vascular fibrosis. Diabetologia 63 (8), 1564–1575. doi:10.1007/s00125-020-05168-7.

Mizuno, A., Noma, Y., Kuwajima, M., Murakami, T., Zhu, M. & Shima, K. (1999). Changes in islet capillary angioarchitecture coincide with impaired B-cell function but not with insulin resistance in male Otsuka-Long-Evans-Tokushima fatty rats: dimorphism of the diabetic phenotype at an advanced age. Metabolism: clinical and experimental 48 (4), 477–483. doi:10.1016/s0026-0495(99)90107-5.

Muzzin, P., Eisensmith, R. C., Copeland, K. C. & Woo, S. L. (1996). Correction of obesity and diabetes in genetically obese mice by leptin gene therapy. Proceedings of the National Academy of Sciences of the United States of America 93 (25), 14804–14808. doi:10.1073/pnas.93.25.14804.

Nakamura, M., Kitamura, H., Konishi, S., Nishimura, M., Ono, J., Ina, K., Shimada, T. & Takaki, R. (1995). The endocrine pancreas of spontaneously diabetic db/db mice: microangiopathy as revealed by transmission electron microscopy. Diabetes research and clinical practice 30 (2), 89–100. doi:10.1016/0168-8227(95)01155-2.

Narayanan, S., Loganathan, G., Dhanasekaran, M., Tucker, W., Patel, A., Subhashree, V., Mokshagundam, S., Hughes, M. G., Williams, S. K. & Balamurugan, A. N. (2017). Intra-islet endothelial cell and β-cell crosstalk: Implication for islet cell transplantation. World journal of transplantation 7 (2), 117–128. doi:10.5500/wjt.v7.i2.117.

Okajima, Y., Matsuzaka, T., Miyazaki, S., Motomura, K., Ohno, H., Sharma, R., Shimura, T., Istiqamah, N., Han, S. I., Mizunoe, Y., Osaki, Y., Iwasaki, H., Yatoh, S., Suzuki, H., Sone, H., Miyamoto, T., Aita, Y., Takeuchi, Y., Sekiya, M., Yahagi, N. … Shimano, H. (2022). Morphological and functional adaptation of pancreatic islet blood vessels to insulin resistance is impaired in diabetic db/db mice. Biochimica et biophysica acta. Molecular basis of disease 1868 (4), 166339. doi:10.1016/j.bbadis.2022.166339.

Olfert, I. M., Baum, O., Hellsten, Y. & Egginton, S. (2016). Advances and challenges in skeletal muscle angiogenesis. American journal of physiology. Heart and circulatory physiology 310 (3), H326–H336. doi:10.1152/ajpheart.00635.2015.

Olver, T. D., Ferguson, B. S. & Laughlin, M. H. (2015). Molecular Mechanisms for Exercise Training-Induced Changes in Vascular Structure and Function. In: C. Bouchard (ed.) Progress in Molecular Biology and Translational Science. 1. Edition. Amsterdam: Elsevier 227-257. doi:10.1016/bs.pmbts.2015.07.017.

Overi, D., Carpino, G., Moretti, M., Franchitto, A., Nevi, L., Onori, P., De Smaele, E., Federici, L., Santorelli, D., Maroder, M., Reid, L. M., Cardinale, V., Alvaro, D. & Gaudio, E. (2022). Islet Regeneration and Pancreatic Duct Glands in Human and Experimental Diabetes. Frontiers in cell and developmental biology 10, 814165. doi:10.3389/fcell.2022.814165.

Paavonsalo, S., Hariharan, S., Lackman, M. H. & Karaman, S. (2020). Capillary Rarefaction in Obesity and Metabolic Diseases-Organ-Specificity and Possible Mechanisms. Cells 9 (12), 2683. doi:10.3390/cells9122683.

Perko, M. J., Nielsen, H. B., Skak, C., Clemmesen, J. O., Schroeder, T. V. & Secher, N. H. (1998). Mesenteric, coeliac and splanchnic blood flow in humans during exercise. The Journal of physiology 513 (Pt 3), 907–913. doi:10.1111/j.1469-7793.1998.907ba.x.

Potente, M. & Mäkinen, T. (2017). Vascular heterogeneity and specialization in development and disease. Nature reviews. Molecular cell biology 18 (8), 477–494. doi:10.1038/nrm.2017.36.

Pugsley, M. K. & Tabrizchi, R. (2000). The vascular system. An overview of structure and function. Journal of pharmacological and toxicological methods 44 (2), 333–340. doi:10.1016/s1056-8719(00)00125-8.

Ramirez-Pedraza, M. & Fernández, M. (2019). Interplay Between Macrophages and Angiogenesis: A Double-Edged Sword in Liver Disease. Frontiers in immunology 10, 2882. doi:10.3389/fimmu.2019.02882.

Reynolds, J. C., Ward, P.J., Martin, J. A., Su, G. L. & Whitcomb D. C. (2016). Pancreas. In: F. H. Netter (ed.) The Netter collection of medical illustrations: Digestive system Part III - Liver, Biliary Tract, and Pancreas. Volume 9. Elsevier, 133–153.

Richards, O. C., Raines, S. M. & Attie, A. D. (2010). The role of blood vessels, endothelial cells, and vascular pericytes in insulin secretion and peripheral insulin action. Endocrine reviews 31 (3), 343–363. doi:10.1210/er.2009-0035.

Richardson, T. M., Saunders, D. C., Haliyur, R., Shrestha, S., Cartailler, J. P., Reinert, R. B., Petronglo, J., Bottino, R., Aramandla, R., Bradley, A. M., Jenkins, R., Phillips, S., Kang, H., Human Pancreas Analysis Program, Caicedo, A., Powers, A. C. & Brissova, M. (2023). Human pancreatic capillaries and nerve fibers persist in type 1 diabetes despite beta cell loss. American journal of physiology. Endocrinology and metabolism 324 (3), E251–E267. doi:10.1152/ajpendo.00246.2022.

Rodrigues, K., Vieira Dias Da Silva, V., Nunes Goulart da Silva Pereira, E., Rangel Silvares, R., Peres de Araujo, B., Eduardo Ilaquita Flores, E., Ramos, I. P., Pereira Borges, J.,

Fernandes-Santos, C. & Daliry, A. (2022). Aerobic Exercise Training Improves Microvascular Function and Oxidative Stress Parameters in Diet-Induced Type 2 Diabetic Mice. Diabetes, metabolic syndrome and obesity : targets and therapy 15, 2991–3005. doi:10.2147/DMSO.S365496.

Rorsman, P. & Ashcroft, F. M. (2018). Pancreatic β-Cell Electrical Activity and Insulin Secretion: Of Mice and Men. Physiological reviews 98 (1), 117–214. doi:10.1152/physrev.00008.2017.

Rugivarodom, M., Geeratragool, T., Pausawasdi, N. & Charatcharoenwitthaya, P. (2022). Fatty Pancreas: Linking Pancreas Pathophysiology to Nonalcoholic Fatty Liver Disease. Journal of clinical and translational hepatology 10 (6), 1229–1239. doi:10.14218/JCTH.2022.00085

Schindelin, J., Arganda-Carreras, I., Frise, E., Kaynig, V., Longair, M., Pietzsch, T. … Cardona, A. (2012). Fiji: an open-source platform for biological-image analysis. Nature Methods 9 (7), 676–682. doi:10.1038/nmeth.2019.

Shah, P., Lueschen, N., Ardestani, A., Oberholzer, J., Olerud, J., Carlsson, P. O. & Maedler, K. (2016). Angiopoetin-2 Signals Do Not Mediate the Hypervascularization of Islets in Type 2 Diabetes. PloS one 11 (9), e0161834. doi:10.1371/journal.pone.0161834.

Shao, Y., Chen, J., Li, X. R. & Ma, J. X. (2020). Detection and Quantification of Retinal Neovascularization Using BrdU Incorporation. Translational vision science & technology 9 (9), 4. doi:10.1167/tvst.9.9.4.

Steiner, D. J., Kim, A., Miller, K. & Hara, M. (2010). Pancreatic islet plasticity: interspecies comparison of islet architecture and composition. Islets 2 (3), 135–145. doi:10.4161/isl.2.3.11815.

Swisa, A., Glaser, B. & Dor, Y. (2017). Metabolic Stress and Compromised Identity of Pancreatic Beta Cells. Frontiers in genetics 8, 21. doi:10.3389/fgene.2017.00021.

Takahashi, K., Mizukami, H., Osonoi, S., Takeuchi, Y., Kudoh, K., Sasaki, T., Daimon, M. & Yagihashi, S. (2021). Islet microangiopathy and augmented β-cell loss in Japanese non-obese type 2 diabetes patients who died of acute myocardial infarction. Journal of diabetes investigation 12 (12), 2149–2161. doi:10.1111/jdi.13601.

Thyfault, J. P. & Bergouignan, A. (2020). Exercise and metabolic health: beyond skeletal muscle. Diabetologia 63 (8), 1464–1474. doi:10.1007/s00125-020-05177-6.

Trimm, E. & Red-Horse, K. (2023). Vascular endothelial cell development and diversity. Nature reviews. Cardiology 20 (3), 197–210. doi:10.1038/s41569-022-00770-1.

Tsai, C. C., Chen, Y. J., Yu, H. R., Huang, L. T., Tain, Y. L., Lin, I. C., Sheen, J. M., Wang, P. W. & Tiao, M. M. (2020). Long term N-acetylcysteine administration rescues liver steatosis via endoplasmic reticulum stress with unfolded protein response in mice. Lipids in health and disease 19 (1), 105. doi:10.1186/s12944-020-01274-y.

Vetterlein, F., Pethö, A. & Schmidt, G. (1987). Morphometric investigation of the microvascular system of pancreatic exocrine and endocrine tissue in the rat. Microvascular research 34 (2), 231–238. doi:10.1016/0026-2862(87)90056-2.

Virtanen, I., Banerjee, M., Palgi, J., Korsgren, O., Lukinius, A., Thornell, L. E., Kikkawa, Y., Sekiguchi, K., Hukkanen, M., Konttinen, Y. T. & Otonkoski, T. (2008). Blood vessels of human islets of Langerhans are surrounded by a double basement membrane. Diabetologia 51 (7), 1181–1191. doi:10.1007/s00125-008-0997-9.

Wang, F., Hull, R. L., Vidal, J., Cnop, M. & Kahn, S. E. (2001). Islet amyloid develops diffusely throughout the pancreas before becoming severe and replacing endocrine cells. Diabetes 50 (11), 2514–2520. doi:10.2337/diabetes.50.11.2514.

Weinberg, S. R., Segev, O., Dor, S. & Raz, I. (2023). Drug Therapies for Diabetes. International journal of molecular sciences 24 (24), 17147. doi:10.3390/ijms242417147.

World Health Organization. (2020). The top ten leading causes of death. Cited 10.5.2024. https://www.who.int/news-room/fact-sheets/detail/the-top-10-causes-of-death.

Xiao, X., Fischbach, S., Fusco, J., Zimmerman, R., Song, Z., Nebres, P., Ricks, D. M., Prasadan, K., Shiota, C., Husain, S. Z. & Gittes, G. K. (2016). PNA lectin for purifying mouse acinar cells from the inflamed pancreas. Scientific reports 6, 21127. doi:10.1038/srep21127.

Zou, Y., Chen, Z., Sun, C., Yang, D., Zhou, Z., Peng, X., Zheng, L. & Tang, C. (2021). Exercise Intervention Mitigates Pathological Liver Changes in NAFLD Zebrafish by Activating SIRT1/AMPK/NRF2 Signaling. International journal of molecular sciences 22 (20), 10940. doi:10.3390/ijms222010940.

APPENDIX 1. Haematoxylin-eosin staining protocol for paraffin sections.

Deparaffinisation

1. Wash 3x5 min with xylene
2. Wash 2x5 min with 100 % ethanol
3. Wash 2x5 min with 90 % ethanol
4. Wash 2x5 min with 80 % ethanol
5. Wash 2x5 min with 70 % ethanol
6. Wash 1x5 min with MilliQ

Staining

1. Put into haematoxylin for 3 min
2. Put under running tap water for 10 min
3. Put into MilliQ for 1 min
4. Put into eosin for 40 seconds

Dehydration

1. Wash quickly with MilliQ
2. Wash quickly with 2x 70 % ethanol
3. Wash quickly with 2x 80 % ethanol
4. Wash quickly with 2x 90 % ethanol
5. Wash quickly with 2x 100 % ethanol
6. Wash quickly with xylene
7. Leave into the second xylene cuvette for 5’

Mounting

1. Mount with xylene based Pertex

APPENDIX 2. Immunofluorescence staining protocol for paraffin embedded tissue sections.

- Fix tissue pieces in 4 % paraformaldehyde (PFA) at 4C for 24 h.
- Processing and paraffin embedding at NOVA hospital molecular pathology lab.
- Cutting paraffin-embedded tissues into 5-10 μm sections

Deparaffinization

1. Wash 3x5 min with xylene
2. Wash 2x5 min with 99,5 % ethanol
3. Wash 2x5 min with 96 % ethanol
4. Wash 1x5 min with 70 % ethanol
5. Wash 1x5 min with milliQ

Antigen retrieval

1. Boil the sections in Tris-EDTA buffer for 15 min in **96˚C**
(Tris-EDTA = 100 mM Tris + 1 mM EDTA + 0.05% Tween20, diluted into PBS, pH=9.0)
2. Cool down on ice for 20 min
3. Wash 2x5 min with PBS
4. Put the section into 0.3 % H_2O_2 in PBS for 30 min in RT

Staining

1. Add blocking solution AND incubate for 1h in RT
(blocking solution = 2.5 % normal donkey serum + 0.2 % bovine serum albumin, in PBS)
2. Add primary antibodies (diluted into blocking solution)

Pancreas	blood vessels	goat-anti-podocalyxin	1:400	R&D Systems	AF1556
	β-cells	rabbit-anti-insulin	1:10 000	Abcam	181547
Liver	blood vessels	goat-anti-podocalyxin	1:400	R&D Systems	AF1556

3. Incubate the sections + primary antibodies for 1h in RT
4. Wash the sections 3x5 min in PBS.
5. Add secondary antibodies (diluted into PBS) for 1h in RT <u>PROTECT FROM LIGHT</u>

Pancreas	blood vessels	555	Donkey-anti-goat IgG	1:500	Invitrogen Alexa Fluor™	CAT# A21432
	β-cells	488	Donkey-anti-rabbit IgG	1:500	Invitrogen Alexa Fluor™	CAT# A21206
	Acinar cells	649	UEA1	1:200	Vector Laboratories	DL-1068-1
Liver	blood vessels	555	Donkey-anti-goat IgG	1:500	Invitrogen Alexa Fluor™	CAT# A21432

6. Wash sections 5 min with PBS
7. Add DAPI, diluted 1:1000 in PBS, for 5 min (also the negative control)
8. Wash sections 5 min with PBS
9. Mount the sections with ProLong Diamond antifade reagent
+ <u>STORE PROTECTED FROM LIGHT</u> at +4C.

APPENDIX 3. Fiji/ImageJ image analysis code for capillaries of pancreas sections.

```
//Brief Description: //
//This script starts by segmenting the 2 tissue compartments (Langerhans islets and exocrine).
//The segmentation of the structures of interest follows, namely the nuclei and the capillaries.
//Finally, the measurements are performed within each compartment. Both in absolute (normalized by area) and in relative terms (capillaries per nuclei, etc).

//**DISCLAIMER**//
//This script is written by Vasco Fachada and Outi Hasu, firstly for the purpose of producing data for Outi's master thesis.
//Any further scientific output using data or results generated by this script or variations of it, should forcibly include both authors of the same script as co-authors.

//First started on May 2024. Last update July 2024

//Principal Investigator: Riikka Kivelä

/////START/////
//setBatchMode(true);
//function to close ROI used often
function closeROI(){
	if(roiManager("size") > 0){
		roiManager("Deselect");
		roiManager("Delete");
	}
	roiManager("Show None");
	//Roi.selectNone;
	close("ROI Manager");
}
//closing all the open images before starting any analysis
while (nImages>0) {
		selectImage(nImages);
	close();
```

```
}
//This closes any additional windows that are not images (tables, ROIs, etc)
list = getList("window.titles");
for (i=0; i<list.length; i++){
	winame = list[i];
	selectWindow(winame);
	print(winame);
	run("Close");
 }
//set working directory
//Finding the files
dir = getDirectory("Select the directory containing the data for your experimental setup (where folder 'raw' is located).");
//dir = "D:"+File.separator+"microscope_room_data"+File.separator+"Eeli"+File.separator+"TraDeRe"+File.separator+"Staining1"+File.separator; //for testing
startTime = getTime();//start timer
folder = "raw";
//folder = "testing"; //comment this line out when you are done testing
rawFiles = getFileList(dir+File.separator+folder);
for (f=0; f<rawFiles.length; f++){
	if (endsWith(rawFiles[f], ".czi") == 0){
		rawFiles = Array.deleteValue(rawFiles, rawFiles[f]);
	}
}
File.makeDirectory(dir+File.separator+"results");
File.makeDirectory(dir+File.separator+"masks");

subjectsFile = dir+File.separator+"results"+File.separator+"Measurements.csv";
if (File.exists(subjectsFile)){
	File.delete(subjectsFile);
}
//Core contents part
for (f=0; f<rawFiles.length; f++){
	id = dir+folder+File.separator+rawFiles[f];
```

```
	filename = substring(rawFiles[f], 0, 6);
	print("processing file "+filename);
	run("Bio-Formats Importer", "open=["+id+"] autoscale color_mode=Default rois_import=[ROI manager] view=Hyperstack stack_order=XYCZT");
	rename("startFILE");
	getPixelSize(unit, pixelWidth, pixelHeight);
	getCompartments(); //both islets and exocrine
	print(filename+"'s compartments now segmented");
	getStructures(); //both capillaries and nuclei
	print(filename+"'s structures now segmented");
	getMeasurements();
	print(filename+"'s measurements now completed");
}
function getCompartments(){
////////////////////////////////////
//Segmenting the islets///
////////////////////////////////////
//Step 1
//there is autofluorescence coming from red blood cells in all channels
//So, subtract capillary (blue, channel 3) signal from islet (green, channel 2) signal, in order signal/noise ratio
	selectImage("startFILE");
	setSlice(3);
	run("Duplicate...", "title=autofluor_capil");
	selectImage("startFILE");
	setSlice(2);
	run("Duplicate...", "title=autofluo_islets");
	imageCalculator("Subtract create", "autofluo_islets","autofluor_capil");
	rename("fluo_subtracted_islet");
	close("autofluo_islets", "autofluor_capil");
	close("autofluor_capil");
	//step 2
	setAutoThreshold("Li dark no-reset");
	//setOption("BlackBackground", true);
```

```
	run("Convert to Mask");
	run("Remove Outliers...", "radius=5 threshold=50 which=Bright");
	run("Maximum...", "radius=15");
	run("Fill Holes");
	run("Minimum...", "radius=10");
//Now we set the measurements to include shape descriptors, then through "analyze particles" add ROIs
	run("Analyze Particles...", "add");
	selectImage("startFILE");
	setSlice(4);
//then iterate each ROI one-by-one
	for (r=0; r<roiManager("count"); r++){
		roiManager("Select", r);
		roiManager("Rename", "tempIslets_"+r);
		//waitForUser("roi #"+r);
		List.setMeasurements;
		if (parseInt(List.getValue("Area")) < 100){ //any binarized pseudo-islet smaller than 100 is to be excluded!
			roiManager("Delete");
			print("roi #"+r+" is a false islet, now deleted!");
			r=r-1;
		}else{
//set a solidity cut-off value of >0.650 for real islets;
//also, real islets have close to zero signal in gray; as opposite to the fake/artifacts large islets which have always some strong gray signal
//...Therefore, any pseudo-islet with a mean gray (channel 4) values over 9, are to be excluded and considered false islets
			if (parseInt(List.getValue("Median")) < 9 && parseInt(List.getValue("Solidity")) >0.5){
				print("roi #"+r+" is a proper islet! Going to be included.");
			}else{
				roiManager("Delete");
				print("roi #"+r+" is a false islet, now deleted!");
				r=r-1;
```

```
                        }
                }
        }
        tempIslets = newArray(roiManager("count"));
        for (i=0; i<tempIslets.length;i++){
                tempIslets[i] = i;
        }
        roiManager("select", tempIslets);
        roiManager("Combine");
        roiManager("Add");
        roiManager("Select", i);
        roiManager("Rename", "combined_islets");
        roiManager("select", tempIslets);
        roiManager("Delete");
        close("fluo_subtracted_islet");
////////////////////////////////////
////EXOCRINE MASK////
////////////////////////////////////
//Now I'm creating a mask for the gray-free zone (empty area where nasty large vessels (blood and others live)
        selectImage("startFILE");
        setSlice(4); //exocrine channel
        roiManager("Deselect");
        roiManager("Show All");
        roiManager("Show None");
        run("Duplicate...", "title=tissueMask");
        run("Duplicate...", "title=vessels");
//first lets segment the large non-blood vessels (which are staining positive for the same marker as the exocrine)
        setAutoThreshold("Yen dark no-reset");
        run("Remove Outliers...", "radius=20 threshold=50 which=Dark");
        run("Analyze Particles...", "size=750-Infinity show=Masks");
        rename("vesselMask");
        run("Create Selection");
```

```
	run("Make Inverse");
//subtract the vessels from the exocrine
	if(selectionType == 1){
		selectImage("tissueMask");
		run("Restore Selection");
		run("Enlarge...", "enlarge=20 pixel");
		run("Clear", "slice")
	}
	close("vesselMask");
	close("vessels");
//now continue to segment the actual exocrine tissue
	selectImage("tissueMask");
	setAutoThreshold("Percentile dark no-reset");
	run("Convert to Mask");
	run("Remove Outliers...", "radius=3 threshold=50 which=Bright");
	run("Remove Outliers...", "radius=50 threshold=50 which=Dark");
	run("Maximum...", "radius=15");
	run("Remove Outliers...", "radius=10 threshold=50 which=Dark");
	setAutoThreshold("MinError dark no-reset");
	run("Convert to Mask");
//But here now you have to exclude the islets (green, channel 2) from the created mask (because you dont want to exclude vessels coming from the islets, only those large ones from the 'interstitium'
	RoiManager.selectByName("combined_islets");
	run("Clear", "slice");
	run("Create Selection");
	roiManager("Add");
	roiManager("Select", roiManager("count")-1);
	roiManager("Rename", "exocrine");
	roiManager("save",   dir+File.separator+"masks"+File.separator+filename+"_compartments.zip");
	close("tissueMask");
}
function getStructures(){
```

```
//////////////////////////////
//DAPI MASK////////
//////////////////////////////
	selectImage("startFILE");
	setSlice(1);
	run("Duplicate...", "title=segmentedDAPI");
	run("Command From Macro", "command=[de.csbdresden.stardist.StarDist2D], args=['input':'segmentedDAPI', 'modelChoice':'Versatile (fluorescent nuclei)', 'normalizeInput':'true', 'percentileBottom':'2.0', 'percentileTop':'100.0', 'probThresh':'0.5', 'nmsThresh':'0.5', 'outputType':'Label Image', 'nTiles':'4', 'excludeBoundary':'1', 'roiPosition':'Automatic', 'verbose':'false', 'showCsbdeepProgress':'false', 'showProbAndDist':'false'], process=[false]");
	rename("labeledNuclei");
	getStatistics(area, mean, min, max, std, histogram);
// Set threshold from 1 to maximum
	setThreshold(1, max);
	run("Convert to Mask");
//run("Invert", "slice");
	run("Watershed");
	setVoxelSize(pixelWidth, pixelHeight, 1, unit);
	run("Duplicate...", "title=isletsNuclei");
	run("Duplicate...", "title=exocrineNuclei");
	selectImage("isletsNuclei");
	RoiManager.selectByName("combined_islets");
	run("Clear Outside");
	selectImage("exocrineNuclei");
	RoiManager.selectByName("exocrine");
	run("Clear Outside");
	close("segmentedDAPI");
	close("labeledNuclei");
//////////////////////////////////////
//CAPILLARIES MASK///
//////////////////////////////////////
	selectImage("startFILE");
```

```
	setSlice(3);
	run("Duplicate...", "title=segmentedCaps");
	setAutoThreshold("Default dark no-reset");
	setOption("BlackBackground", true);
	run("Convert to Mask");
	run("Despeckle");
	run("Fill Holes");
	run("Duplicate...", "title=isletsCaps");
	run("Duplicate...", "title=exocrineCaps");
	selectImage("isletsCaps");
	RoiManager.selectByName("combined_islets");
	run("Clear Outside");
	selectImage("exocrineCaps");
	RoiManager.selectByName("exocrine");
	run("Clear Outside");
	close("segmentedCaps");
	close("startFILE");
}
function getMeasurements(){
////////////////////////////////////////////////
//////////MEASUREMENTS//////////
////////////////////////////////////////////////
// Now we have the real islets, lets start measuring stuff
	run("Set Measurements...", "area mean shape feret's redirect=None decimal=3");
//measure islet area and islet nuclei number
	selectImage("isletsNuclei");
	List.setMeasurements;
	TotIsletArea = parseFloat(List.getValue("Area")); //total ROI area
	run("Analyze Particles...", "summarize");
	selectWindow("Summary");
	IJ.renameResults("Summary","Results");
	IslNucNum = getResult("Count", 0);
	close("Results");
//measure exocrine area and exocrine nuclei number
```

```
        selectImage("exocrineNuclei");
        List.setMeasurements;
        TotExoArea = parseFloat(List.getValue("Area")); //total ROI area
        run("Analyze Particles...", "summarize");
        selectWindow("Summary");
        IJ.renameResults("Summary","Results");
        ExoNucNum = getResult("Count", 0);
        close("Results");
//measure islet capillaries
        selectImage("isletsCaps");
        run("Analyze Particles...", "summarize");
        selectWindow("Summary");
        IJ.renameResults("Summary","Results");
        IslCapsNum = getResult("Count", 0)/TotIsletArea;
        IslCapsArea = getResult("Total Area", 0)/TotIsletArea;
        IslCapsNucRatio = getResult("Count", 0)/IslNucNum;
        IslCapsFeret = getResult("Feret", 0);
        close("Results");
//measure exocrine capillaries
        selectImage("exocrineCaps");
        run("Analyze Particles...", "summarize");
        selectWindow("Summary");
        IJ.renameResults("Summary","Results");
        ExoCapsNum = getResult("Count", 0)/TotExoArea;
        ExoCapsArea = getResult("Total Area", 0)/TotExoArea;
        ExoCapsNucRatio = getResult("Count", 0)/ExoNucNum;
        ExoCapsFeret = getResult("Feret", 0);
        close("Results");
//Create datafile in case there is none
        if (!File.exists(subjectsFile)){
// Create a header
        File.append("sample,total_islet_area,total_exocrine_area,number_of_capillar-
ies_per_islet_area,capillaries_total_area_per_islet_area,number_of_capillaries_per_num-
```

```
ber_of_nuclei_in_islets,capillary_feret_in_islets,number_of_capillaries_per_exo-
crine_area,capillaries_total_area_per_exocrine_area,number_of_capillaries_per_num-
ber_of_nuclei_in_exocrine,capillary_feret_in_exocrine", subjectsFile);
        }
// insert data into table
        File.append(filename+","+TotIsletArea+","+TotExoArea+","+IslCap-
sNum+","+IslCapsArea+","+IslCapsNucRatio+","+IslCapsFeret+","+ExoCapsNum+","+Exo-
CapsArea+","+ExoCapsNucRatio+","+ExoCapsFeret, subjectsFile);
//ASSEMBLE LAST COMPOSITE AND SAVE IT
        run("Merge Channels...", "c1=isletsCaps c3=isletsNuclei c5=exocrineNuclei c6=exo-
crineCaps create");
        saveAs("Tiff", dir+"results"+File.separator+substring(rawFiles[f], 0, lengthOf(raw-
Files[f])-4)+"_CLASSIFIED");
        close();
        closeROI();
}
```